NATIONAL ADVISORY COMMITTEE FOR AERONAUTICS

REPORT 1309

AERODYNAMIC CHARACTERISTICS AT HIGH SPEEDS OF RELATED FULL-SCALE PROPELLERS HAVING DIFFERENT BLADE-SECTION CAMBERS

By JULIAN D. MAYNARD and LELAND B. SALTERS, Jr.

1957

For sale by the Superintendent of Documents, U. S. Government Printing Office, Washington 25, D. C. Yearly subscription, $10; foreign, $11.25; single copy price varies according to size - - - - - - - - - Price 30 cents

REPORT 1309

AERODYNAMIC CHARACTERISTICS AT HIGH SPEEDS OF RELATED FULL-SCALE PROPELLERS HAVING DIFFERENT BLADE-SECTION CAMBERS

By JULIAN D. MAYNARD and LELAND B. SALTERS, Jr.

Langley Aeronautical Laboratory

Langley Field, Va.

National Advisory Committee for Aeronautics

Headquarters, 1512 H Street NW., Washington 25, D. C.

Created by Act of Congress approved March 3, 1915, for the supervision and direction of the scientific study of the problems of flight (U. S. Code, title 50, sec. 151). Its membership was increased from 12 to 15 by act approved March 2, 1929, and to 17 by act approved May 25, 1948. The members are appointed by the President and serve as such without compensation.

REPORT 1309

AERODYNAMIC CHARACTERISTICS AT HIGH SPEEDS OF RELATED FULL-SCALE PROPELLERS HAVING DIFFERENT BLADE-SECTION CAMBERS [1]

By Julian D. Maynard and Leland B. Salters, Jr.

SUMMARY

Wind-tunnel tests of a full-scale two-blade NACA 10–(10)(08)–03 (high camber) propeller have been made for a range of blade angles from 20° to 55° at airspeeds up to 500 miles per hour. The results of these tests have been compared with results from previous tests of the NACA 10–(3)(08)–03 (low camber) and NACA 10–(5)(08)–03 (medium camber) propellers to evaluate the effects of blade-section camber on propeller aerodynamic characteristics.

Maximum propeller efficiency for cruise and high-speed conditions of operation at subcritical Mach numbers is indicated for blades having a design lift coefficient (design camber) at the 0.7 radius of 0.45 to 0.60, provided NACA 16-series sections are used. Although blades with higher design lift coefficients have a lower maximum efficiency, they have a more extensive range of thrust coefficients for efficient operation. At the design operating condition the high-camber propeller produced 80 percent more thrust and absorbed 83 percent more power than the low-camber propeller. Because of its high power-absorption qualities the propeller with a high design lift coefficient is much more efficient for take-off and climb conditions of operation than propellers with low design lift coefficients. The blade-section design lift coefficient of the NACA 16-series airfoils may be increased up to a value of 1.0 at the 0.7 radius with the attainment of maximum propeller efficiencies as high as 90 percent if the helical tip Mach number is kept below 0.85.

At helical tip Mach numbers up to 1.14 the maximum efficiency at the design blade angle of 45° is higher for the low-camber and medium-camber propellers than for the high-camber propeller. The high-camber propeller, however, is useful for conditions of operation at which high thrust is required at moderate speeds. The critical tip Mach number is lowered by an increase in blade-section design camber, but the supercritical tip Mach number at which recovery of thrust occurs is lower for the high-camber propeller than for the low-camber propeller.

INTRODUCTION

A general investigation of the aerodynamic characteristics of a series of full-scale 10-foot-diameter propellers is being made in the Langley 16-foot high-speed tunnel. The purpose of the investigation is to determine the combined influence of propeller-design parameters and compressibility upon propeller performance. The blade designs embody systematic variations in blade width, thickness ratio, shank form, blade airfoil section, and design lift coefficient or camber. All the blades were designed to operate with a minimum induced-energy loss when the blade angle at the 0.7 radius is 45° and the blade is operating at an advance ratio of 2.1.

The first results of the full-scale propeller tests are given in references 1 and 2, which present the aerodynamic characteristics of the NACA 10-(3)(08)-03 and NACA 10–(5)(08)–03 propellers. This report presents the aerodynamic characteristics of the NACA 10–(10)(08)–03 propeller and completes the investigation of related propellers differing in blade-section design lift coefficient or camber. The purpose of the present report is to make a comparison of the performance data for the NACA 10–(10)(08)–03 propeller with the data contained in references 1 and 2 to afford an evaluation of the effects of blade-section camber on propeller aerodynamic characteristics. A comparison is also made with the results of model-propeller tests presented in reference 3.

The selection of blade-section camber is of increasing importance in the design of propellers for high speeds because of the penalties in take-off and climb performance incurred by a reduction in camber to obtain higher critical Mach numbers for the blade sections. Limitations of the testing equipment prevent a complete and thorough analysis of the problem. The brief analysis presented herein includes only the primary effects of camber on propeller performance.

SYMBOLS

b	blade width, ft
C_P	propeller power coefficient, $\frac{P}{\rho n^3 D^5}$
C_T	propeller thrust coefficient, $\frac{T}{\rho n^2 D^4}$
c_l	blade-section lift coefficient
c_{l_d}	blade-section design lift coefficient
D	propeller diameter, ft
h	blade-section maximum thickness, ft
J	propeller advance ratio, V/nD
M	air-stream Mach number
M_t	helical tip Mach number, $M\sqrt{1+\left(\frac{\pi}{J}\right)^2}$
n	propeller rotational speed, rps

[1] Supersedes declassified NACA Research Memorandum L8E06 by Julian D. Maynard and Leland B. Salters, Jr., 1948.

P power absorbed by propeller, ft-lb/sec

Δp difference between local pressure at point on airfoil surface and static pressure in undisturbed stream, lb/sq ft

q dynamic pressure, lb/sq ft

$\Delta p/q$ pressure coefficient

T propeller thrust, lb

V airspeed, fps

x fraction of propeller tip radius

α angle of attack, deg

β blade angle at any radius, deg

$\beta_{0.75R}$ blade angle at 0.75 tip radius, deg

η propeller efficiency, $J\frac{C_T}{C_P}$

ρ mass density of air, slugs/cu ft

APPARATUS

PROPELLER DYNAMOMETER

The dynamometer used to test the propellers is powered by two 1000-horsepower electric motors arranged in tandem and coupled for the present tests to allow the power of both motors to be expended through a single propeller. A variable-frequency power supply affords an accurate speed control from 300 to 2100 rpm with a permissible overspeed up to 2280 rpm. Photographs of the dynamometer are shown in figures 1 and 2, and a diagram showing the important dimensions of the propeller dynamometer and its location with respect to the Langley 16-foot-tunnel test section is shown in figure 3. A detailed description of all the test apparatus and the methods of measuring thrust and torque is presented in reference 1. The fairing profile was calculated from a distribution of sources and sinks to produce a body of revolution with uniform axial velocity in the plane of the propeller. This axial-velocity distribution has been checked experimentally and found to be uniform within 1 percent. The gap between the propeller blade and the spinner surface at the juncture of the propeller blade and spinner is very small (fig. 1) but is not sealed.

PROPELLER BLADES

The NACA design numbers are descriptive of the shape, size, and aerodynamic characteristics of the blades used in this investigation. The digits of the first group of numbers represent the propeller diameter in feet; the number in the first parentheses is ten times the basic design lift coefficient at the 0.7 radius; the number in the second parentheses is the thickness ratio (in hundredths) at the 0.7 radius; and the digits in the third group give the solidity of one blade (in hundredths or thousandths for two or three digits, respectively) expressed as the ratio of the blade chord at the 0.7 radius to the circumference of the circle having a radius 0.7 of the propeller-tip radius.

The blades used in the investigation of blade-section camber are the NACA 10–(3)(08)–03 (low camber), NACA 10–(5)(08)–03 (medium camber), and NACA 10–(10)(08)–03 (high camber). These blades are identical except for the difference in blade-section design lift coefficient or camber and a slight difference in pitch distribution as shown in figure 4, which gives the blade-form curves. Figure 5 is a photograph of a typical set of the test blades. The NACA 16-series blade sections (ref. 4) were used, and efficient airfoil sections extend to the spinner which has a diameter 21.7 percent of the diameter of a 10-foot propeller.

Figure 6 shows the blade section and theoretical pressure distribution at the 0.7 radius for each blade design. The theoretical pressure distributions were computed for a lift coefficient of 0.5 by the method described in reference 5. The angle of attack (shown in fig. 6) corresponding to this lift coefficient is different for each blade design and gives some indication of changes in airfoil characteristics caused by the different cambers. Obviously, the high peak pressures caused by operating these airfoils at lift coefficients for which they were not designed would be expected to lower the critical Mach number and seriously affect efficient operation at high speeds.

TESTS AND REDUCTION OF DATA

Thrust, torque, and rotational speed were measured during tests at fixed blade angles of 20°, 25°, 30°, 35°, 40°, 45°, 50°, and 55° at the three-quarter blade (45-inch) radius. A constant rotational speed was used for most of the tests, and a range of advance ratio $\left(J=\frac{V}{nD}\right)$ was covered by changing the tunnel airspeed, which could be varied from about 60 to 500 miles per hour. The range of blade angles covered at the various rotational speeds used in the tests of the NACA 10–(10)(08)–03 propeller is shown in table I. Similar information, together with figure numbers, is also shown in table I for the NACA 10–(3)(08)–03 and NACA 10–(5)(08)–03 propellers as taken from references 1 and 2. At the higher blade angles, the complete range of advance ratio could not be covered at the higher rotational speeds

TABLE I

RANGE OF BLADE ANGLE AND ROTATIONAL SPEED FOR NACA PROPELLER TESTS

Figure	Rotational speed, rpm	Blade angle at 0.75 radius, $\beta_{0.75R}$, deg							
NACA 10–(10)(08)–03 propeller									
7	1140	20	25	30	35	40	45	50	55
8	1350	20	25	30	35	40	45	50	
9	1500						45		
10	1600	20	25	30	35	40	45		
11	2000	20	25	30	35				
12	2160	20	25	30					
13	Varied						45		
NACA 10–(5)(08)–03 propeller (figs. cited are from ref. 2)									
8	1140				35	40	45	50	55
9	1350	20	25	30	35	40	45	50	
10	1500						45		
11	1600	20	25	30	35	40	45		
12	1800	20	25	30	35	40			
13	2000	20	25	30	35				
14	2100	20	25	30					
15	2160	20	25	30					
16	Varied						45		
NACA 10–(3)(08)–03 propeller (figs. cited are from ref. 1)									
19	1140			30	35	40	45	50	55
20	1350	20	25	30	35	40	45	50	
21	1500						45		
22	1600	20	25	30	35	40	45		
23	2000	20	25	30	35				
24	2160	20	25	30					
25	Varied						45		

because of power limitations. In order to obtain propeller characteristics at maximum tunnel airspeeds, a blade angle (45°) was chosen for which the peak-efficiency operating condition could be attained when the tunnel airspeed was at or near the maximum and the dynamometer was operating at its maximum power and rotational speed. For these tests, at a blade angle of 45° the rotational speed was varied to obtain data from the peak-efficiency condition to the zero-torque operating condition.

The test data have been corrected for tunnel-wall interference and for forces acting on the spinner by the methods described in reference 1 and are presented in the form of the usual thrust and power coefficients and propeller efficiency. Propeller thrust, as used herein, is defined as the shaft tension caused by the spinner-to-tip part of the blades rotating in the air stream. Tests were frequently repeated during the test program, and the results obtained agreed with the results presented within 1 percent. For purposes of comparison, therefore, the data are considered accurate to within 1 percent, and the faired envelopes are believed to be accurate to within much closer limits.

RESULTS AND DISCUSSION

CHARACTERISTICS OF THE NACA 10–(10)(08)–03 PROPELLER

Faired curves of thrust coefficient, power coefficient, and propeller efficiency plotted against advance ratio are presented in figures 7 to 13 for the two-blade NACA 10–(10)(08)–03 propeller. Test points are shown in the figures for thrust and power coefficients. The variation of air-stream Mach number and helical tip Mach number with advance ratio is shown in the figures for the propeller efficiency.

The envelope curves of propeller efficiency at the different test rotational speeds are shown in figure 14 for the two-blade NACA 10–(10)(08)–03 propeller. The curves for this propeller show high efficiencies at the lower rotational speeds where the adverse effects of compressibility are small. At a rotational speed of 1140 rpm, the envelope efficiency is above 0.90 for a range of advance ratio from 1.6 to 3.2. At the higher rotational speeds the envelope efficiencies become less, and at 2160 rpm the maximum efficiency reached is about 0.75 at an advance ratio of 0.9.

In figure 15 the envelope efficiency of the two-blade NACA 10–(10)(08)–03 propeller at a rotational speed of 1350 rpm is compared with the optimum efficiency of a two-blade propeller with the Betz minimum induced-energy-loss loading. The curve of optimum efficiency was calculated by a method neglecting all profile-drag losses (ref. 6) for a two-blade propeller operating at the same values of power coefficient as were obtained with the NACA 10–(10)(08)–03 propeller. The curves in figure 15 indicate that the induced losses amount to about 6 percent and the profile-drag losses amount to about 3 percent at the advance ratio of 2.1 to 2.2 for which the propeller was designed. The highest efficiency (approximately 0.91) reflects the importance of designing for a minimum induced-energy-loss loading and of using efficient airfoil sections from the spinner surface to the propeller tip.

Results from tests of the full-scale propeller are compared in figure 16 with results from the tests of a model propeller (NACA 4–(10)(08)–03) presented in reference 3. This comparison shows that, over a range of advance ratio from 0.8 to 2.1, the difference in envelope efficiency for the model and full-scale propellers is 1 percent or less and is perhaps within the limits of experimental accuracy of the two sets of data.

EFFECT OF CAMBER ON PROPELLER EFFICIENCY, POWER, AND THRUST

The envelope efficiencies of the NACA 10–(3)(08)–03 (low camber), NACA 10–(5)(08)–03 (medium camber), and NACA 10–(10)(08)–03 (high camber) propellers are compared in figure 17 for a rotational speed of 1350 rpm. Comparisons at other rotational speeds are similar (except at the highest speeds) and are therefore not shown. The curves in figure 17 show that the medium-camber propeller has the highest envelope efficiency over most of the range of advance ratio, and the high-camber propeller has the lowest envelope efficiency over the entire range of advance ratio. The medium-camber propeller is 2½ to 3 percent more efficient than the low-camber propeller near the design value of advance ratio, and the high-camber propeller is 1½ to 2 percent less efficient than the low-camber propeller near the design value of advance ratio.

A comparison of the three propellers based solely on envelope efficiency may be misleading, however, because of their different power-absorption qualities. As pointed out in reference 3, the primary effect of using propeller blades of increased design camber (increased design lift coefficient) is to increase the power absorbed by the blades as well as to increase the thrust. This increase in thrust and power is illustrated in figure 18 which shows the thrust and power coefficients of the three propellers at a blade angle of 45° and a rotational speed of 1350 rpm. At this rotational speed and an advance ratio (2.2) near the design value, the medium-camber propeller absorbs 30 percent more power and produces 33 percent more thrust than the low-camber propeller. For the same operating condition the high-camber propeller absorbs 83 percent more power and produces 80 percent more thrust than the low-camber propeller. These large increases in power absorption and thrust for the high-camber propeller are produced with no increase in propeller weight and with efficiency losses compared with the medium-camber and low-camber propellers of only 4 and 1½ percent, respectively.

The fact that the medium-camber propeller is more efficient than either the low-camber or high-camber propellers indicates the possibility of a propeller with an optimum design camber. Figure 19 shows the variation of the thrust and power coefficients and the efficiency of the test propellers with the design lift coefficient at the 0.7 radius. For a rotational speed of 1350 rpm and a design blade angle of 45° (fig. 19(a)) maximum efficiency is indicated for blades having a design lift coefficient at the 0.7 radius of 0.45 to 0.60, provided NACA 16-series sections are used. However, for cases in which high power absorption is desired it may be necessary to use higher design lift coefficients. The adverse effects of compressibility, which must also be kept in mind, are indi-

cated by the curves in figure 19(a) for operation at a constant rotational speed of 1600 rpm.

For conditions of operation in which the blade sections are likely to be stalled, the use of highly cambered blade sections is very efficacious. Figure 19(b) shows the effect of design lift coefficient on the propeller characteristics for operation at a blade angle of 35°, a rotational speed of 1140 rpm, and an advance ratio of 1.1. For this climb condition of operation, the medium-camber propeller absorbs 5.4 percent more power, produces 10 percent more thrust, and is about 4 percent more efficient than the low-camber propeller. The high-camber propeller absorbs 24 percent more power, produces 31 percent more thrust, and is 5 percent more efficient than the low-camber propeller. For the condition of operation shown in figure 19(b), the highest efficiency is indicated for blades having a design lift coefficient at the 0.7 radius of 0.75 to 0.95, provided NACA 16-series sections are used. The curves in figure 19 indicate the importance of choosing the correct blade-section camber to meet operational requirements.

A consideration of the theoretical pressure distributions shown in figure 6 indicates that maximum efficiency for operation at a given lift coefficient should occur when the section has a design lift coefficient equal to the operating lift coefficient. This fact is shown to be true by a single-station analysis of camber effects presented in reference 3 and explains the increase in efficiency with increase in design camber for conditions of operation such as take-off and climb where high lift coefficients are necessary. Figure 20 shows the variation of efficiency with thrust coefficient for the test propellers at a rotational speed of 1140 rpm and a blade angle of 45°. These curves show the range of thrust coefficient for efficient operation for each of the blade designs. Although the high-camber propeller has a lower maximum efficiency, it has an extensive range of thrust coefficients for efficient operation. This result may be explained by the fact that blade sections with high design camber can operate at high lift coefficients at much lower angles of attack than blade sections with low design camber; thus stalled conditions may be eliminated. The blade sections with low design camber must operate at high angles of attack to produce high thrust coefficients and may become stalled; the profile-drag losses are thus increased.

EFFECT OF CAMBER ON CONSTANT-POWER PROPELLER OPERATION

Airplane propellers often operate over an extensive range of advance ratio at constant rotational speed and torque. Since blade-section design camber affects the power-absorption qualities of a propeller, the data have been analyzed at several values of constant-power coefficient for a rotational speed of 1140 rpm. The results of this analysis, presented in figure 21, provide a better comparison of the efficiency of the three test propellers than one based on advance ratio alone. For constant values of the power coefficient from 0.1 to 0.2 the medium-camber propeller is the most efficient for the greatest range of advance ratio. However, at low values of advance ratio corresponding to take-off and climb, the high-camber propeller is the most efficient, particularly at the higher power coefficients. For a power coefficient of 0.15 (0.075 per blade) and an advance ratio of 1.1 (fig. 21(b)), the high-camber propeller has an efficiency of 83.5 percent. The corresponding efficiency for the medium-camber propeller is only 76.5 percent.

In general, the high-camber propeller is more efficient than the medium-camber propeller up to values of advance ratio approximately 10 times the value of the power coefficient, and this result is in agreement with results obtained in the model tests of reference 3. The medium-camber propeller is more efficient than the low-camber propeller up to an advance ratio of 3.4 for a power coefficient of 0.1 (fig. 21(a)), but the efficiency of the higher cambered propeller is reduced at high advance ratios. These results show that a compromise must be made in the selection of blade-section design camber to obtain the highest overall efficiency. A blade-section design lift coefficient between 0.5 and 1.0 is indicated, but the adverse effects of compressibility encountered at high speeds may demand a lower camber.

EFFECT OF COMPRESSIBILITY ON PROPELLER CHARACTERISTICS

The familiar loss in maximum efficiency due to compressibility is shown in figure 22 for the three test propellers at a blade angle of 45°. The medium-camber propeller is the most efficient up to a helical tip Mach number of 0.9. From a helical tip Mach number of 0.9 to 1.14 the efficiency of both the low-camber and medium-camber propellers drops from 0.92 to approximately 0.72. The high-camber propeller has the lowest efficiency over the entire range of helical tip Mach numbers; its efficiency drops from 0.90 to 0.73 over a range of helical tip Mach number from 0.85 to 1.03. This low efficiency of the high-camber propeller prevents its use for efficient high-speed operation.

Since the lower efficiency of the high-camber propeller might be due in part to the higher power absorbed, a comparison based on equal power absorption was made. This comparison is shown in figure 23 for a power coefficient of 0.13 and illustrates again the superiority of the low-camber and medium-camber propellers for high helical tip speeds. The power coefficient for maximum efficiency of the high-camber propeller is considerably higher than 0.13, however, and the comparison made in figure 23 favors the low-camber and medium-camber propellers. If a higher power coefficient had been chosen for this comparison, the low-camber and medium-camber propellers would have to operate at high angles of attack, which tends to cause earlier and more extensive compressibility losses. Because of the power limitations previously mentioned, a comparison could not be made at high helical tip speeds for constant-power coefficients higher than 0.13. However, a consideration of the curves in figures 10(c) and 19(a) for a rotational speed of 1600 rpm indicates that a propeller having a design lift coefficient (at the 0.7 radius) of 0.8 might have a high efficiency at fairly high Mach numbers. The interpolated values show that such a propeller could operate at a helical tip Mach number of about 0.94 (air-stream Mach number of 0.54) with a thrust coefficient of 0.069, a power coefficient of 0.169, and an efficiency of 0.90. This result shows that the large power-absorbing qualities of high-camber propellers make them

useful for conditions of operation at which high thrust is required at moderate speeds.

An examination of the thrust and power coefficients of propellers operating when the effects of compressibility are present should provide a better understanding of the problem. In figure 24 the thrust and power coefficients for maximum efficiency are plotted against helical tip Mach number for the three test propellers at a blade angle of 45°. Although the scarcity of data prevents a definite establishment of the critical Mach numbers, the curves in figure 24 were drawn to illustrate the trends indicated by the data. The curves are somewhat similar to plots of the variation of airfoil lift coefficient with Mach number for constant angles of attack and show that increases in thrust and power coefficient occur just before the critical Mach number is reached. After the critical Mach number is reached, there is a marked decrease in both thrust and power coefficients up to a helical tip Mach number of approximately 1.0. At this helical tip Mach number near 1.0 the thrust and power coefficients begin to increase again. It is interesting to note that, although the curves in figure 24 show that the critical tip Mach number is lowered by an increase in blade-section design camber, the Mach number at which recovery of thrust occurs is lower for the high-camber propeller than for the low-camber propeller.

The increases in thrust and power coefficients which occur before the critical Mach number is reached may be utilized to improve take-off characteristics, because for this condition of operation a large portion of the blade operates at relatively high Mach numbers even at low forward speeds. However, increasing the blade-section design camber is a more effective means of improving both the take-off and climb characteristics of propellers. The results (fig. 22) show that the blade-section design lift coefficient may be increased up to a value of 1.0 at the 0.7 radius with the attainment of maximum propeller efficiencies as high as 90 percent if the helical tip Mach number is kept below 0.85. It should be kept in mind, however, that these results apply only to propellers having a minimum induced-energy-loss loading with efficient airfoil sections extending inboard to the spinner surface.

CONCLUSIONS

Wind-tunnel tests of a full-scale two-blade NACA 10–(10)(08)–03 (high camber) propeller have been made for a range of blade angles from 20° to 55° at airspeeds up to 500 miles per hour. The results of these tests and comparisons with results obtained from previous tests of the NACA 10–(3)(08)–03 (low camber) and NACA 10–(5)(08)–03 (medium camber) propellers led to the following conclusions:

1. Increasing the blade-section camber is a very effective means of increasing the thrust and power coefficients of a propeller. At a rotational speed of 1350 rpm near the design condition of operation (blade angle at 0.75 radius equal to 45° and advance ratio equal to 2.2) the medium-camber propeller absorbed 30 percent more power and produced 33 percent more thrust than the low-camber propeller. For the same operating condition, the high-camber propeller absorbed 83 percent more power and produced 80 percent more thrust than the low-camber propeller.

2. For cruise and high-speed conditions of operation at subcritical Mach numbers, maximum propeller efficiency is indicated for blades having a design lift coefficient (design camber) at the 0.7 radius of 0.45 to 0.60, provided NACA 16-series sections are used. Although blades with higher design lift coefficients have a lower maximum efficiency, they have a more extensive range of thrust coefficients for efficient operation.

3. For take-off and climb conditions of operation at low advance ratios and Mach numbers, the propeller with a high design lift coefficient is much more efficient than the propeller with lower design lift coefficients. For a power coefficient of 0.15 (0.075 per blade) and an advance ratio of 1.1, the high-camber propeller has an efficiency of 83.5 percent. The corresponding efficiency for the medium-camber propeller is only 76.5 percent.

4. The blade-section design lift coefficient of the NACA 16-series airfoils may be increased up to a value of 1.0 at the 0.7 radius with the attainment of maximum propeller efficiencies as high as 90 percent if the helical tip Mach number is kept below 0.85.

5. At helical tip Mach numbers up to 1.14 the maximum efficiency at the design blade angle of 45° is higher for the low-camber and medium-camber propellers than for the high-camber propeller. The high-camber propeller, however, is useful for conditions of operation at which high thrust is required at moderate speeds.

6. The critical tip Mach number is lowered by an increase in blade-section design camber, but the supercritical tip Mach number at which recovery of thrust occurs is lower for the high-camber propeller than for the low-camber propeller.

LANGLEY AERONAUTICAL LABORATORY
NATIONAL ADVISORY COMMITTEE FOR AERONAUTICS
LANGLEY FIELD, VA., *May 6, 1948.*

REFERENCES

1. Corson, Blake W., Jr., and Maynard, Julian D.: The Langley 2000-Horsepower Propeller Dynamometer and Tests at High Speed of an NACA 10–(3)(08)–03 Two-Blade Propeller. NACA TN 2859, 1952. (Supersedes NACA RM L7L29, 1948.)
2. Maynard, Julian D.: Aerodynamic Characteristics at High Speeds of Full-Scale Propellers Having Different Shank Designs. NACA RM L6L27a, 1947.
3. Delano, James B.: Investigation of the NACA 4–(5)(08)–03 and NACA 4–(10)(08)–03 Two-Blade Propellers at Forward Mach Numbers to 0.725 To Determine the Effects of Camber and Compressibility on Performance. NACA Rep. 1012, 1951. (Supersedes NACA ACR L5F15.)
4. Stack, John: Tests of Airfoils Designed to Delay the Compressibility Burble. NACA Rep. 763, 1943. (Supersedes NACA TN 976.)
5. Theodorsen, T., and Garrick, I. E.: General Potential Theory of Arbitrary Wing Sections. NACA Rep. 452, 1933.
6. Crigler, John L., and Talkin, Herbert W.: Charts for Determining Propeller Efficiency. NACA WR L–144, 1944. (Formerly NACA ACR L4I29.)

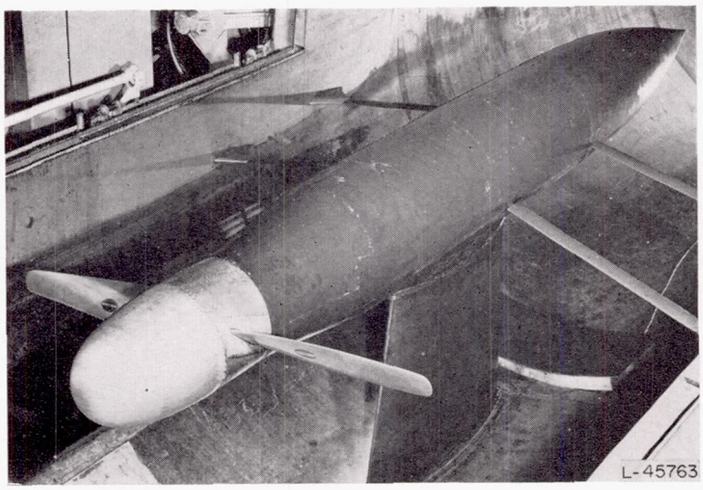

FIGURE 1.—Propeller dynamometer in test section with tunnel open.

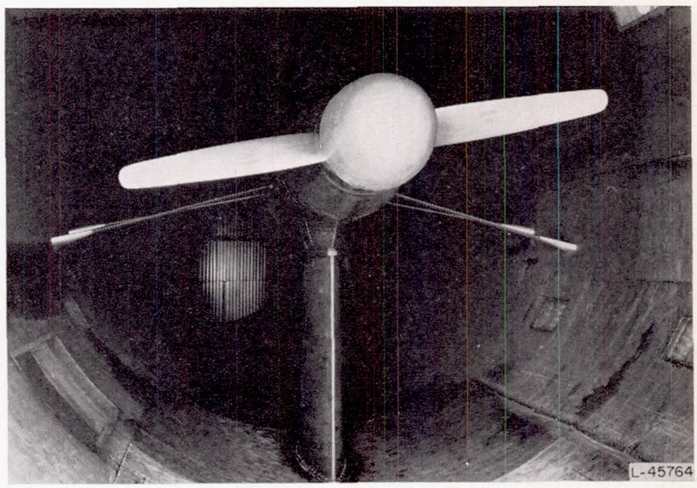

FIGURE 2.—Propeller dynamometer in test section with tunnel closed.

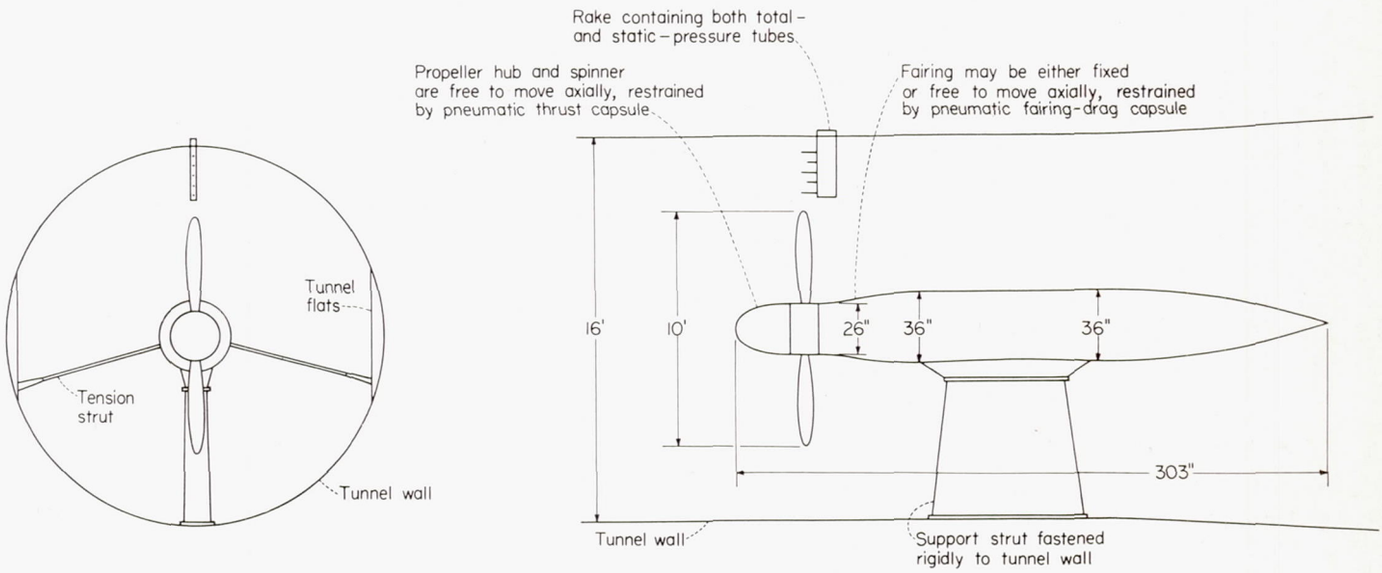

FIGURE 3.—Configuration of 2000-horsepower dynamometer for tests of propellers in the Langley 16-foot high-speed tunnel.

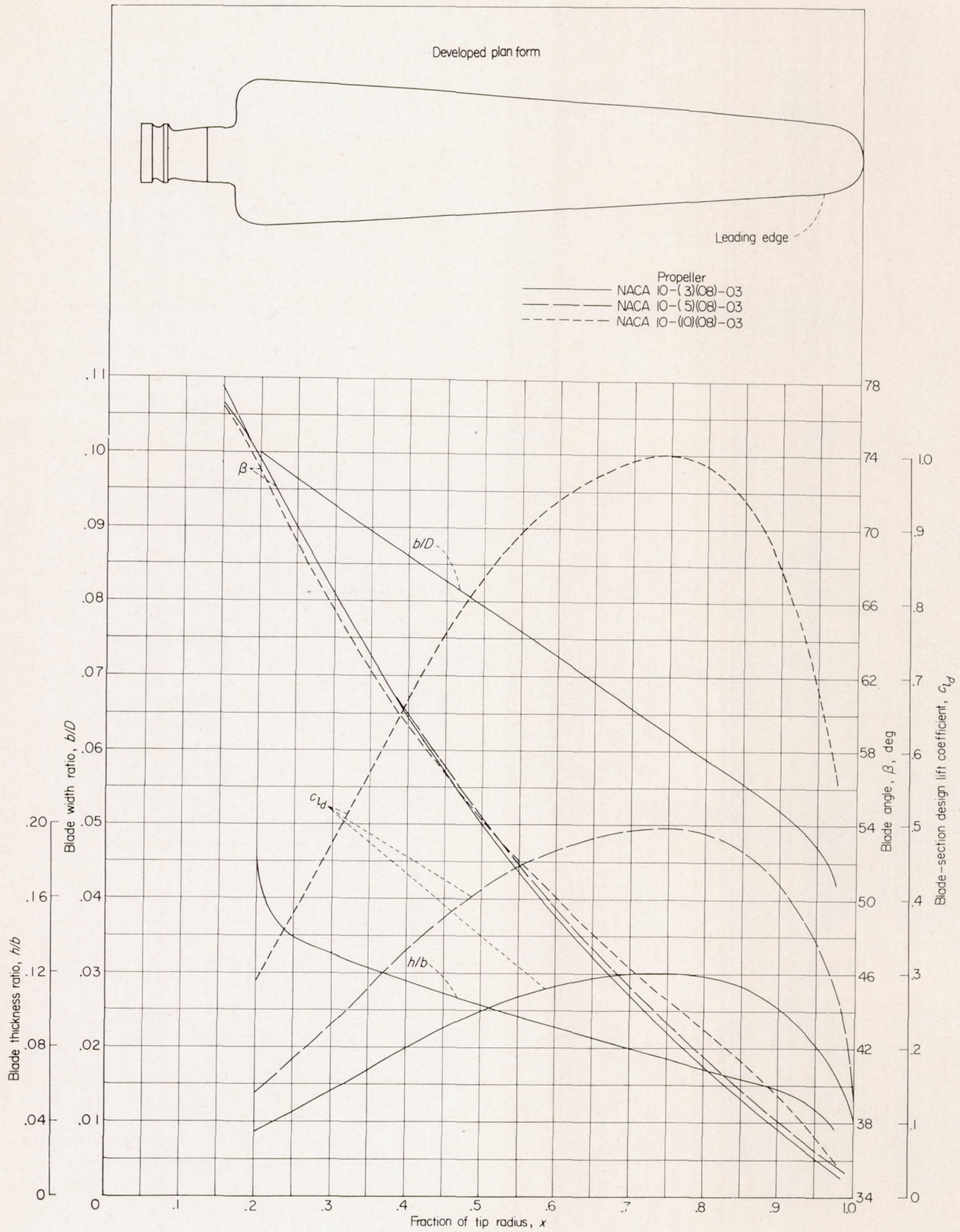

FIGURE 4.—Blade-form curves for NACA propellers.

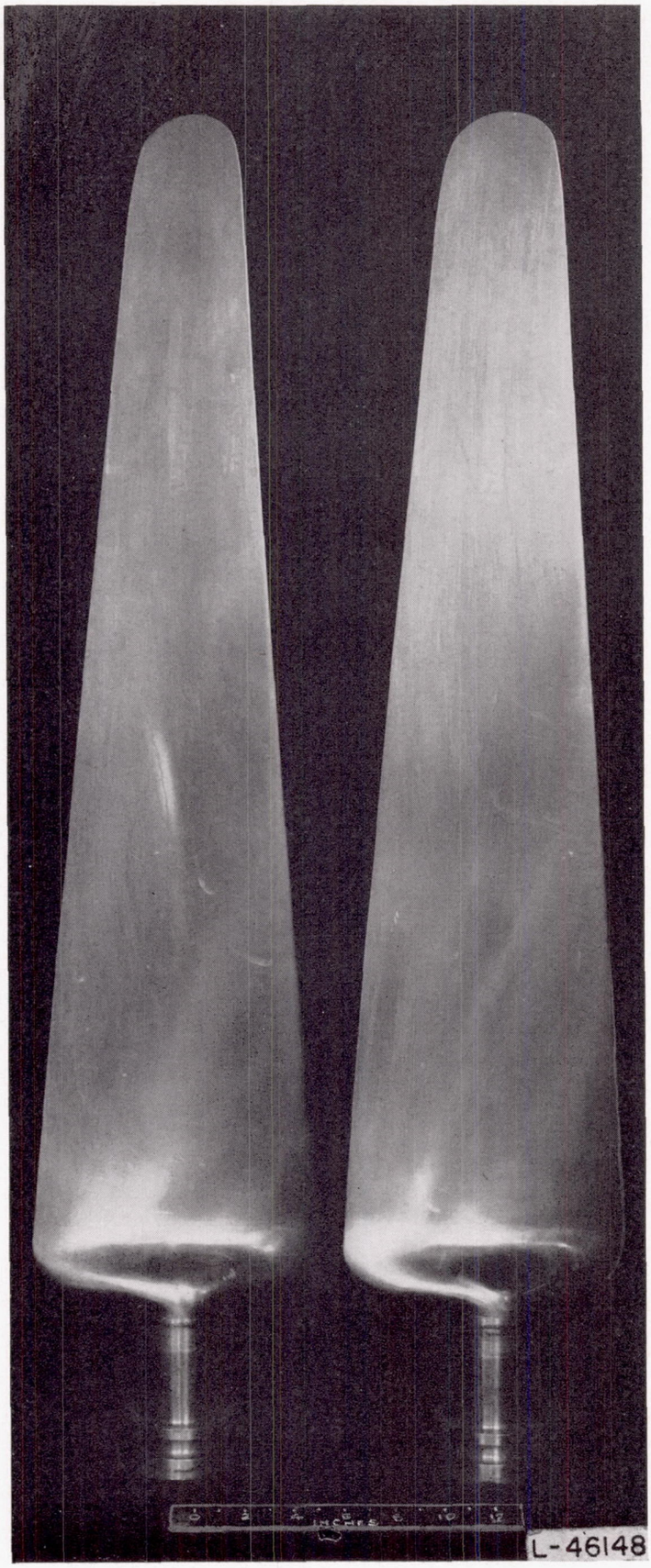

FIGURE 5.—Typical test blades.

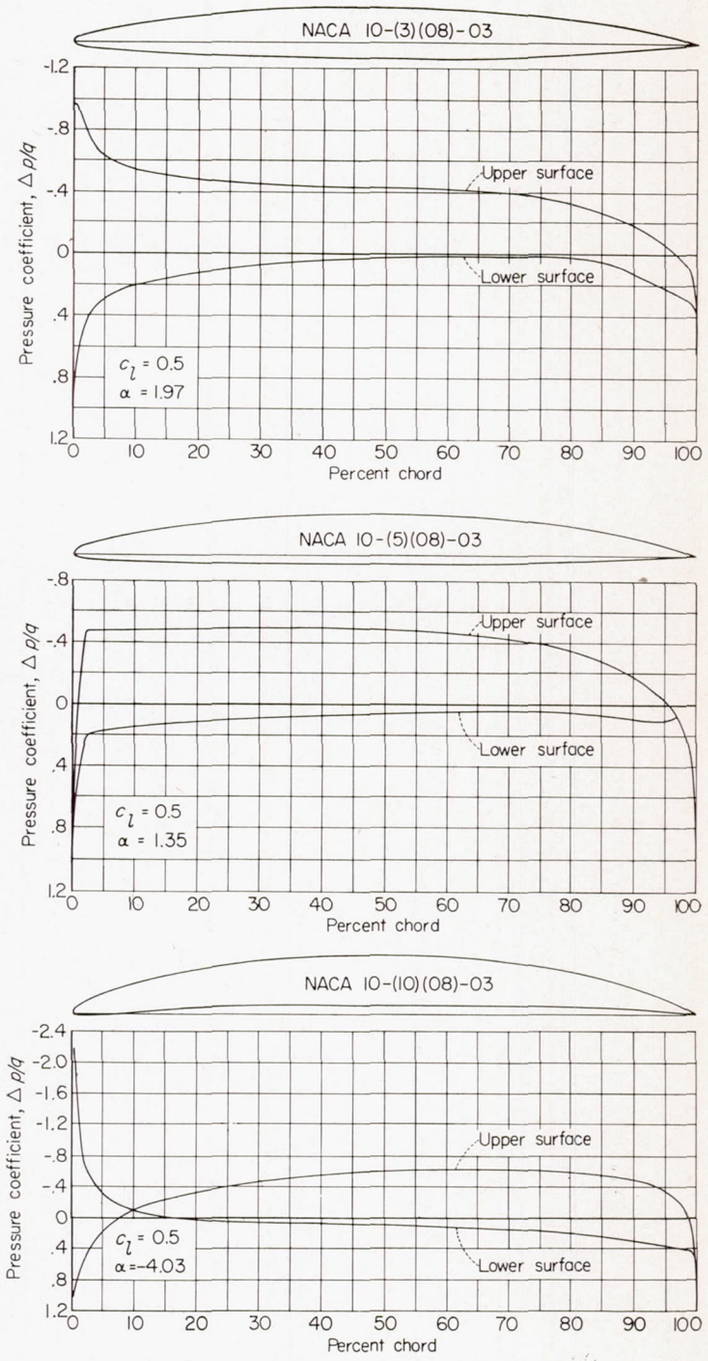

FIGURE 6.—Blade section and theoretical pressure distribution at the 0.7 radius for each propeller design.

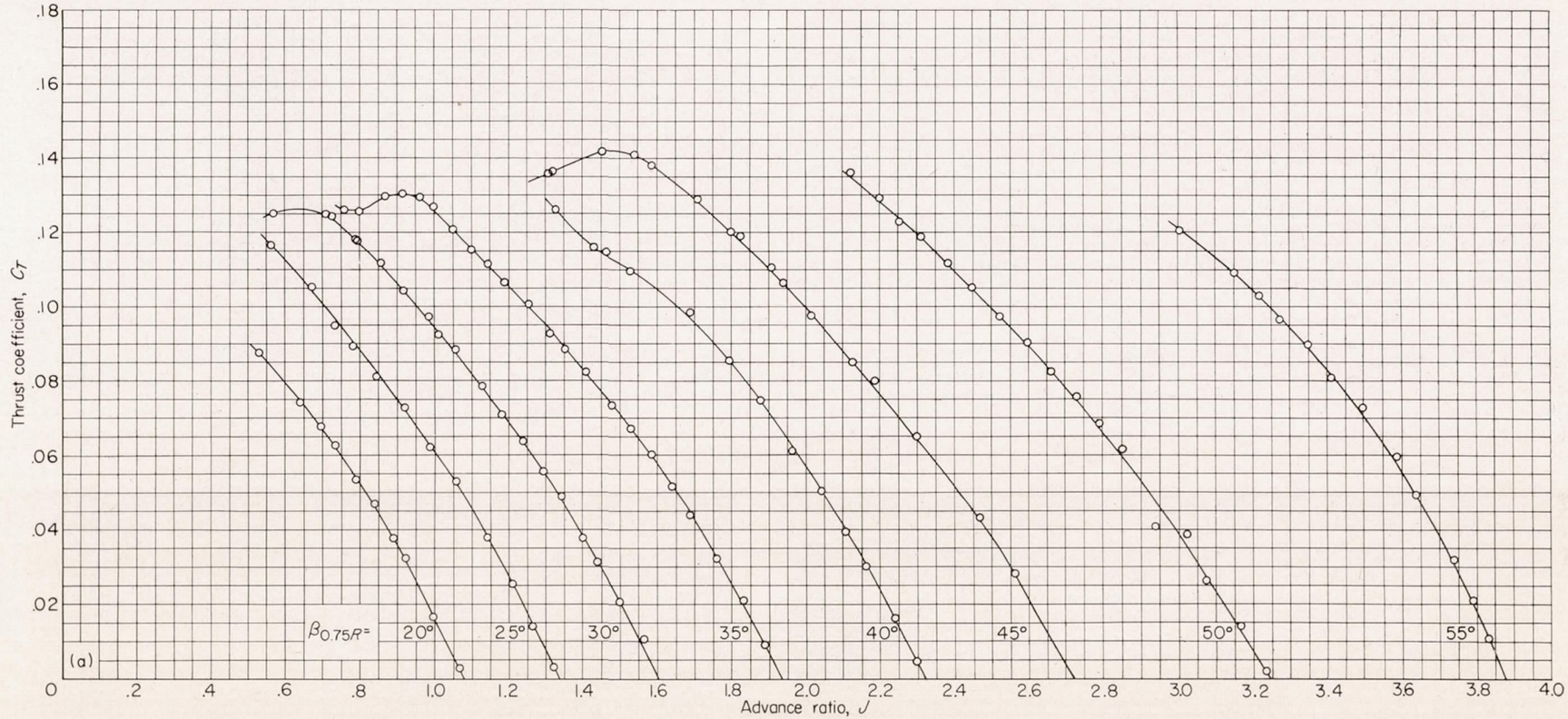

(a) Thrust coefficient.

FIGURE 7.—Characteristics of NACA 10–(10)(08)–03 propeller. Rotational speed, 1140 rpm.

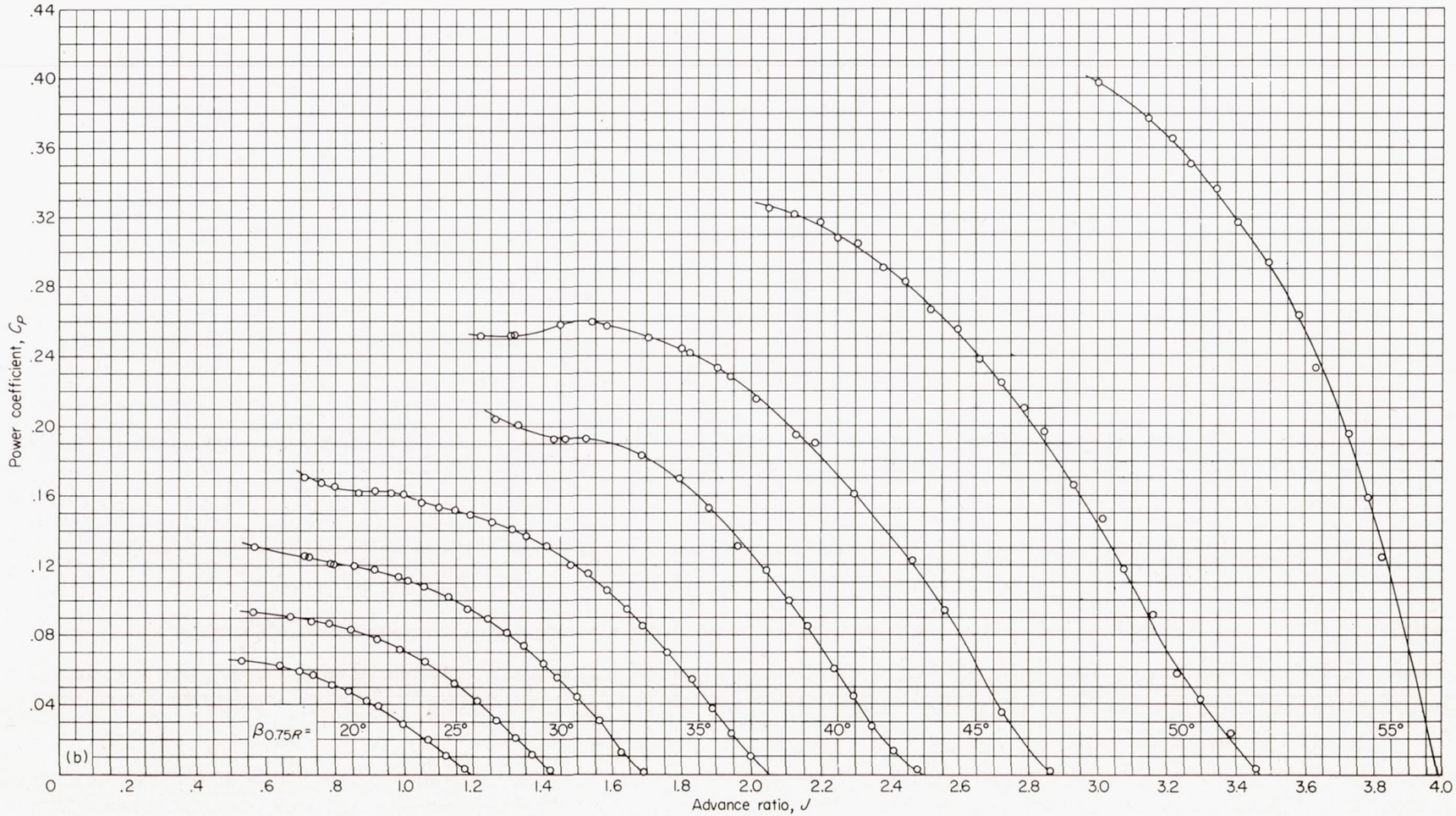

(b) Power coefficient.

FIGURE 7.—Continued.

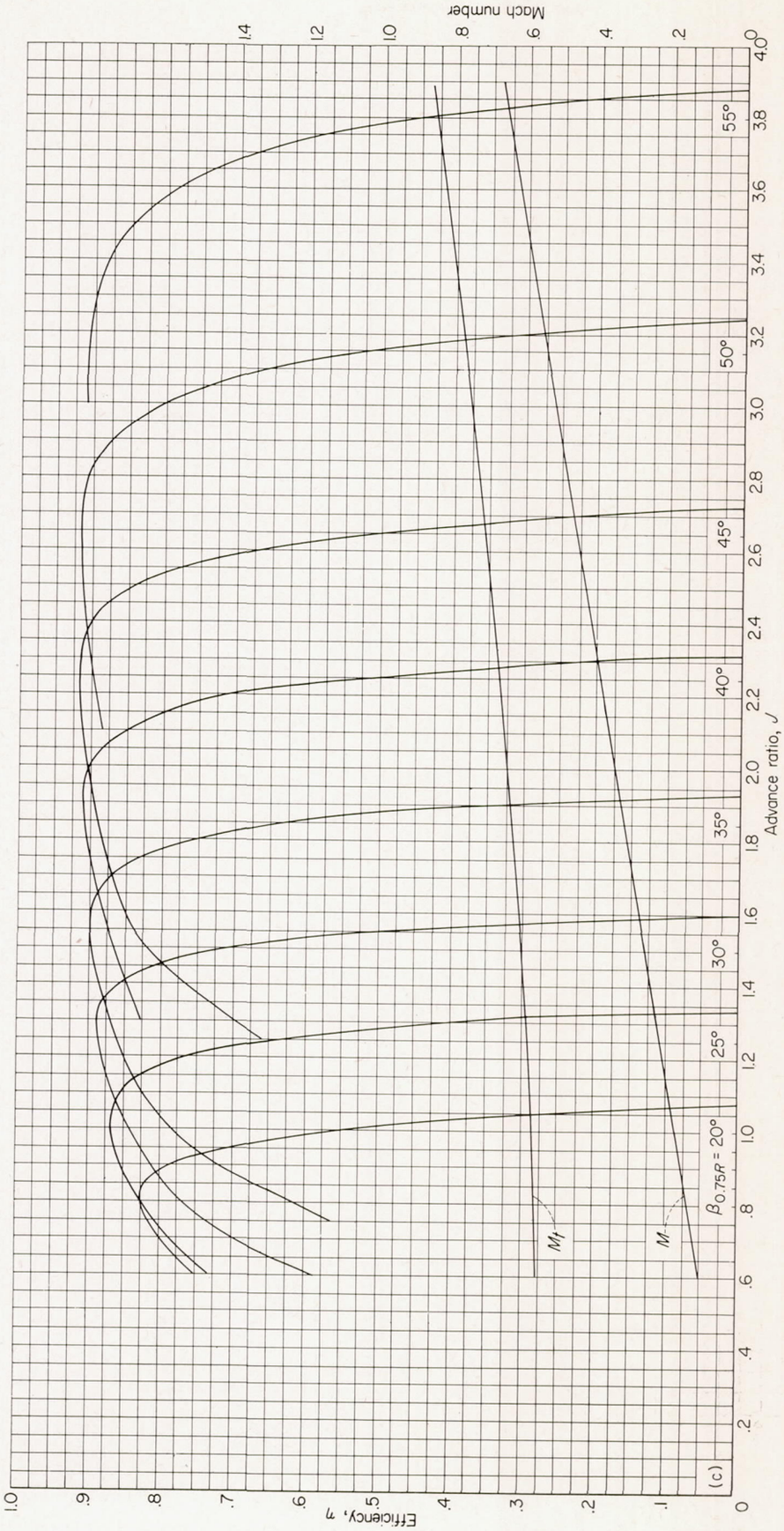

(c) Efficiency.

FIGURE 7.—Concluded.

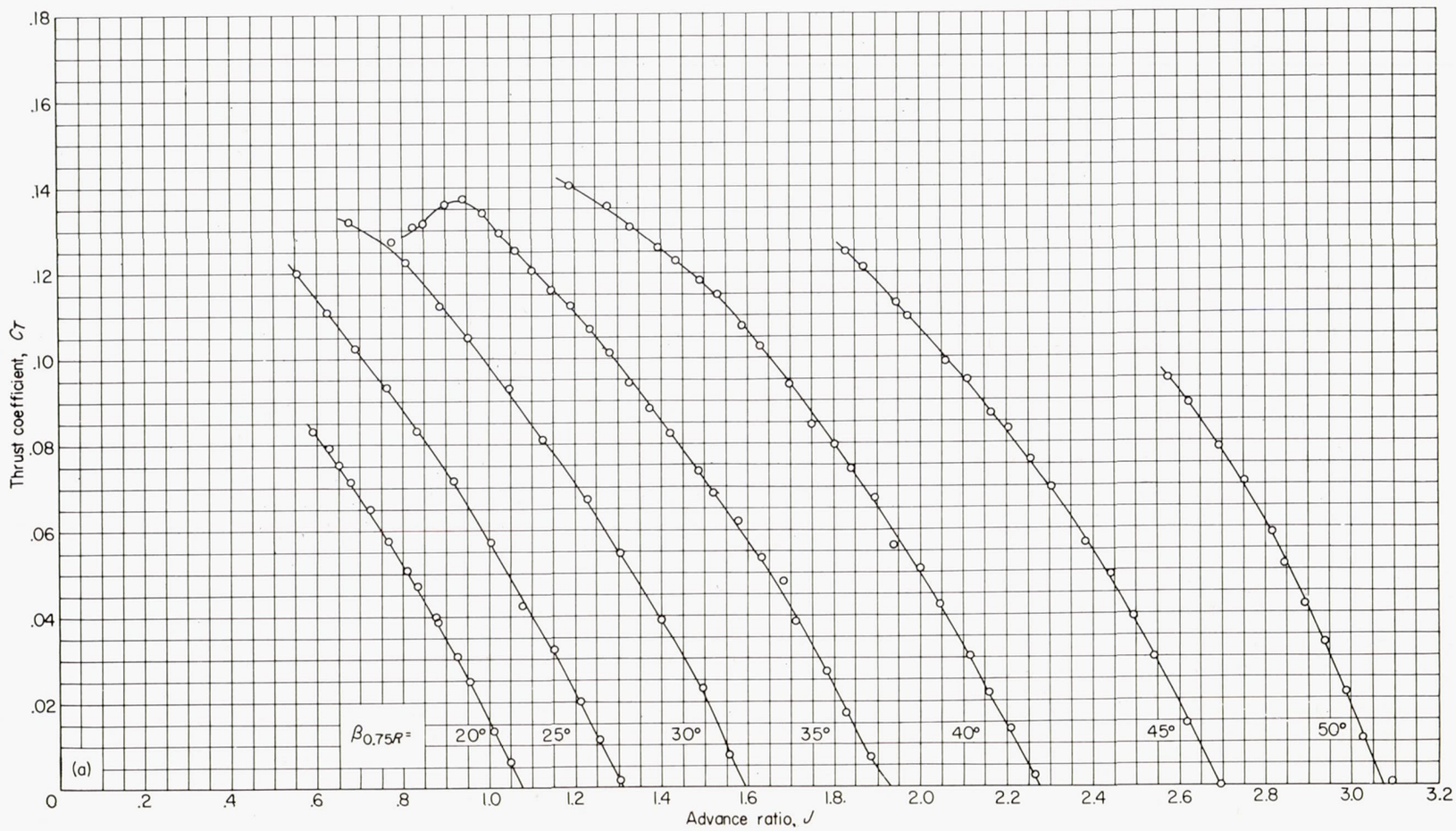

(a) Thrust coefficient.

FIGURE 8.—Characteristics of NACA 10–(10)(08)–03 propeller. Rotational speed, 1350 rpm.

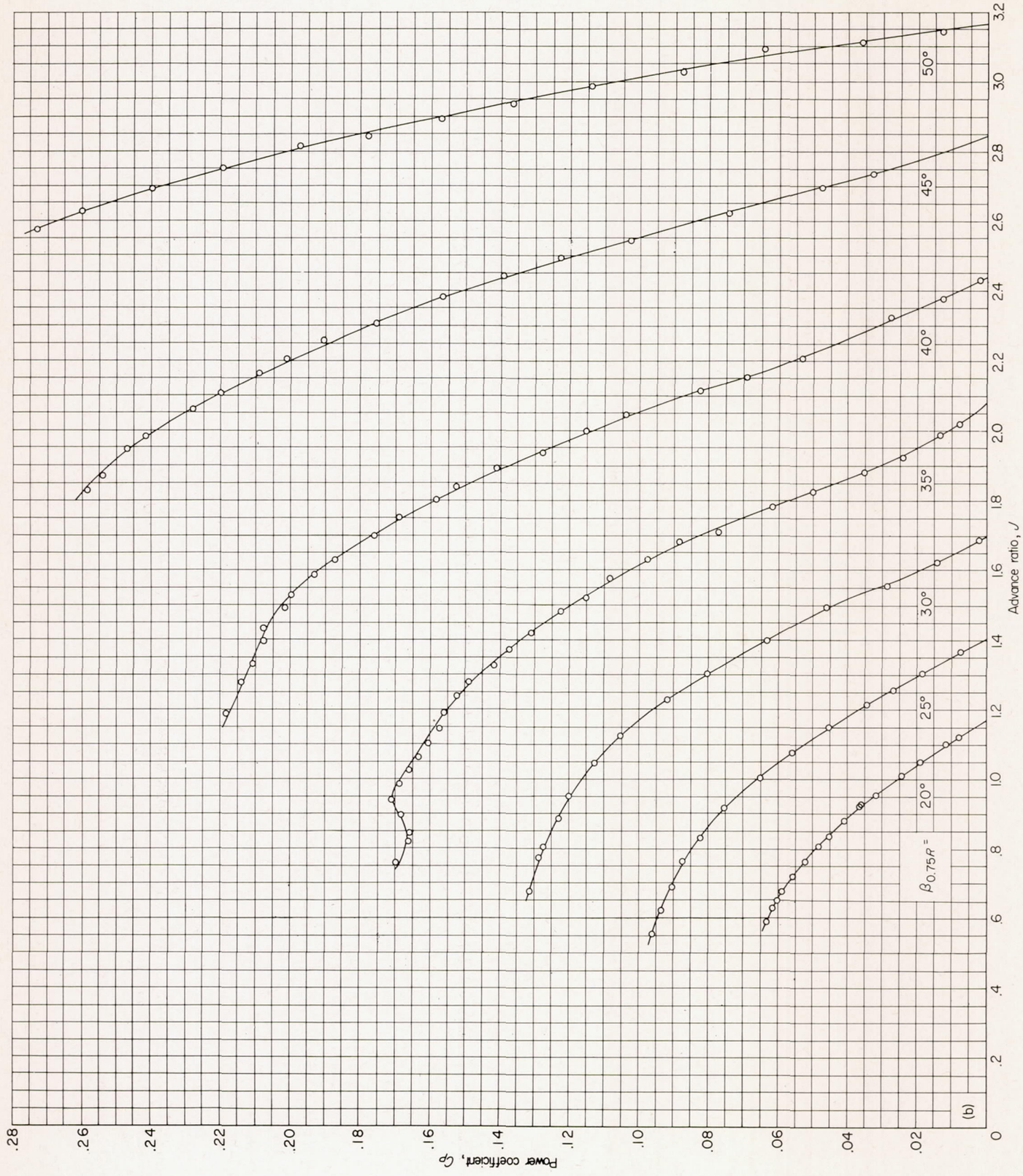

(b) Power coefficient.

FIGURE 8.—Continued

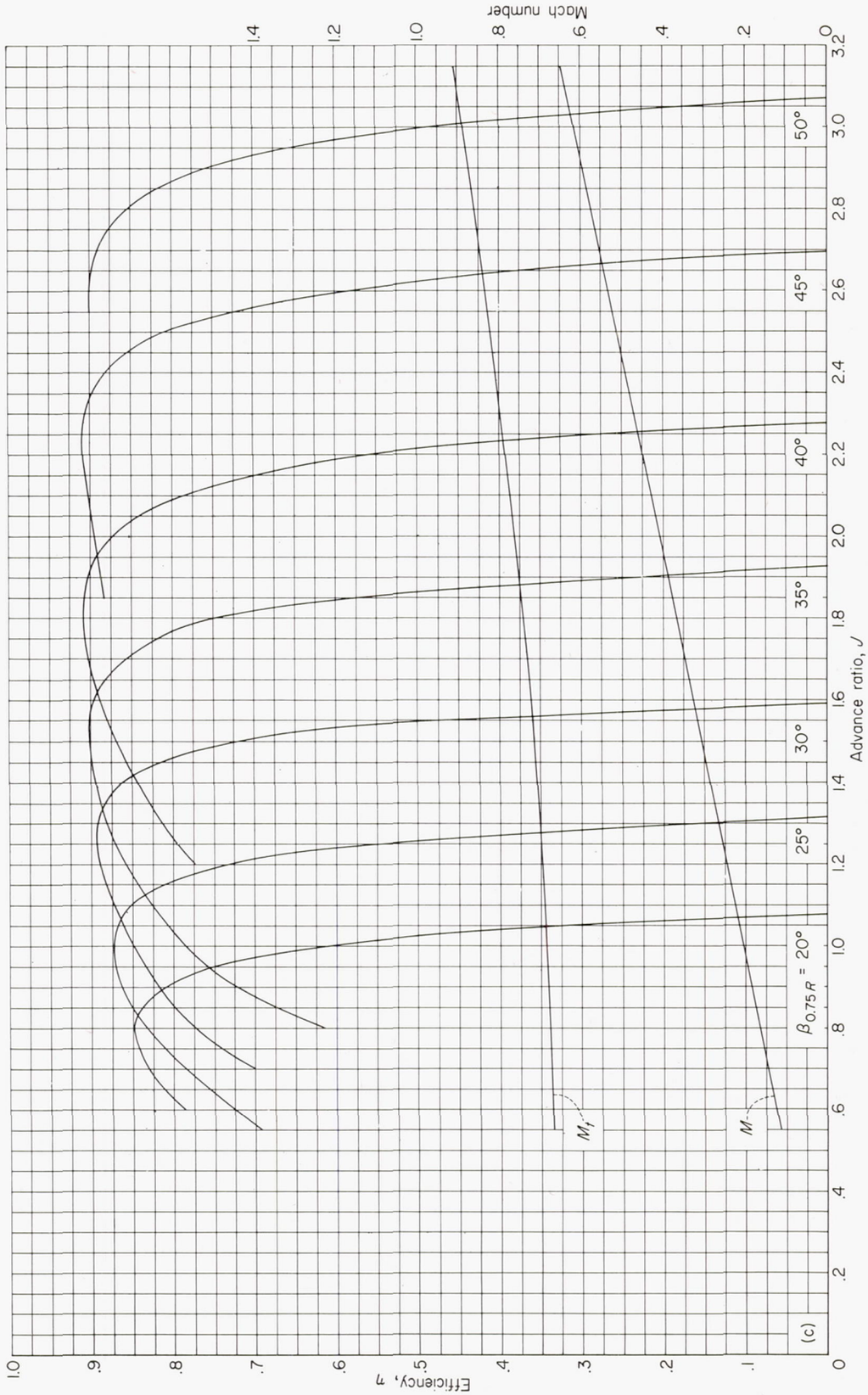

(c) Efficiency.

FIGURE 8.—Concluded.

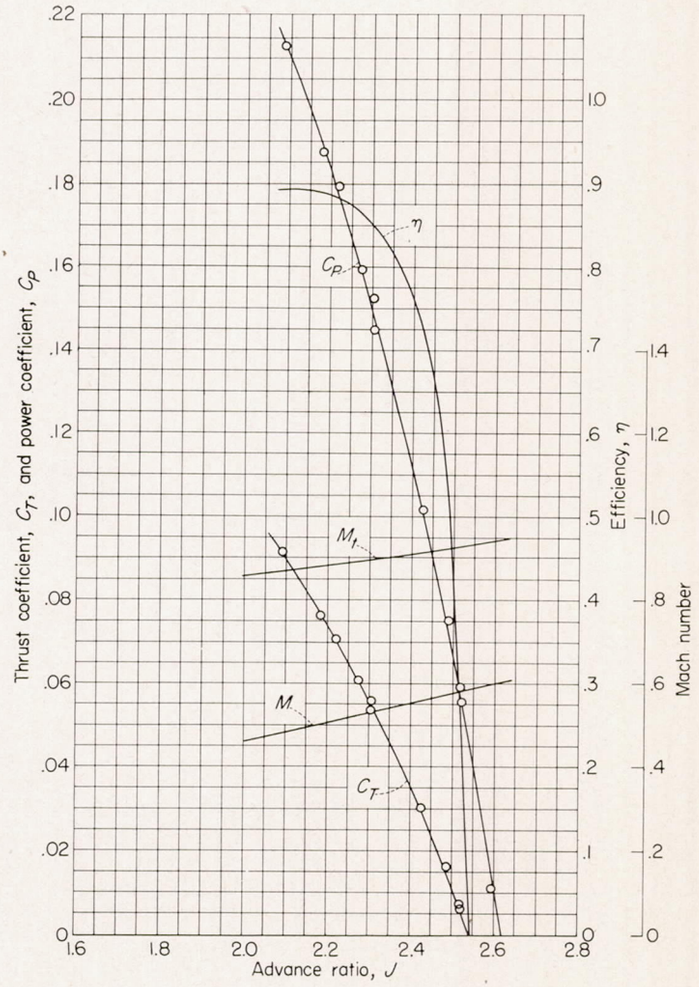

FIGURE 9.—Characteristics of NACA 10–(10)(08)–03 propeller. Rotational speed, 1500 rpm; $\beta_{0.75R}=45°$.

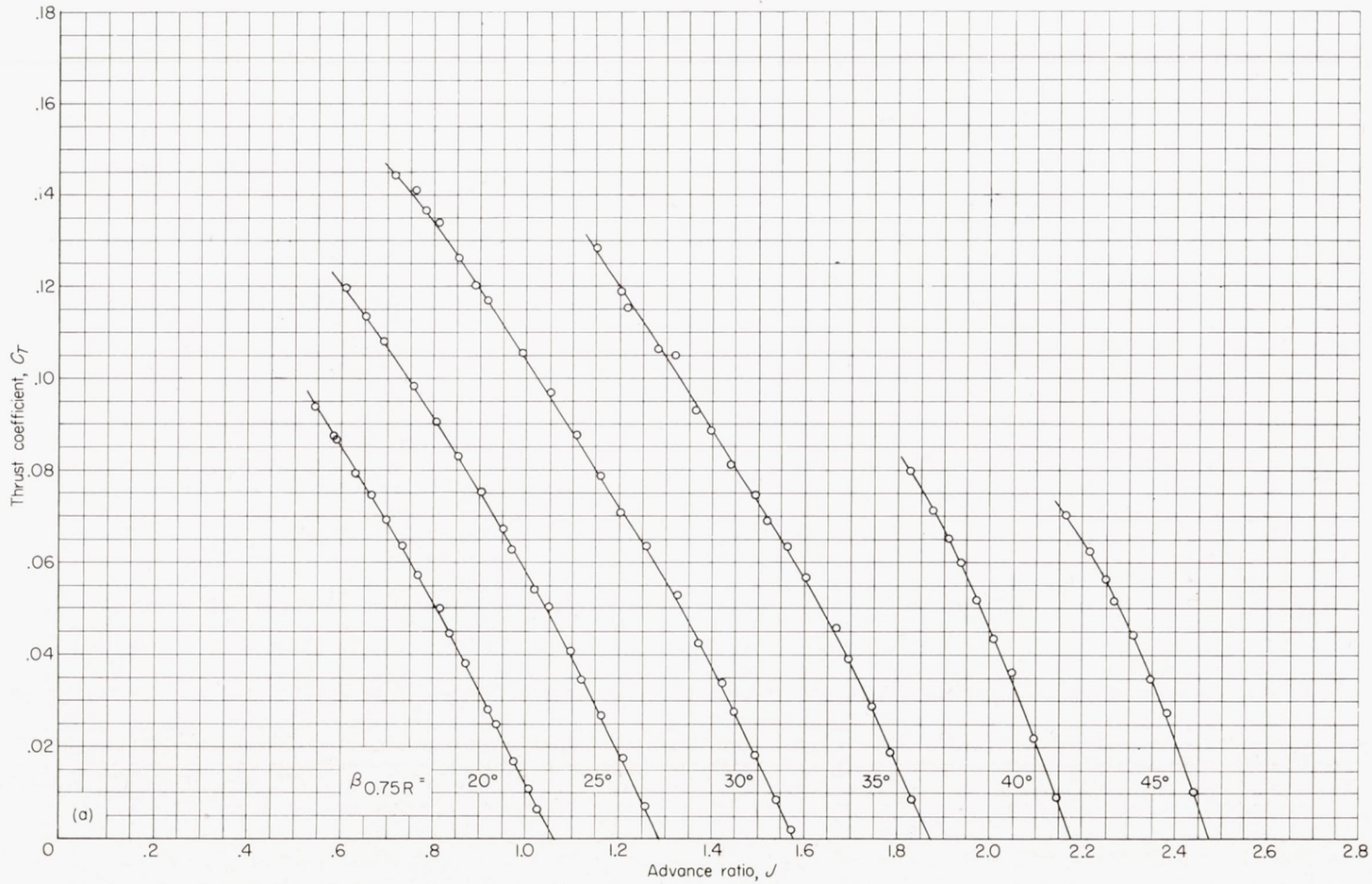

(a) Thrust coefficient.

FIGURE 10.—Characteristics of NACA 10–(10)(08)–03 propeller. Rotational speed, 1600 rpm.

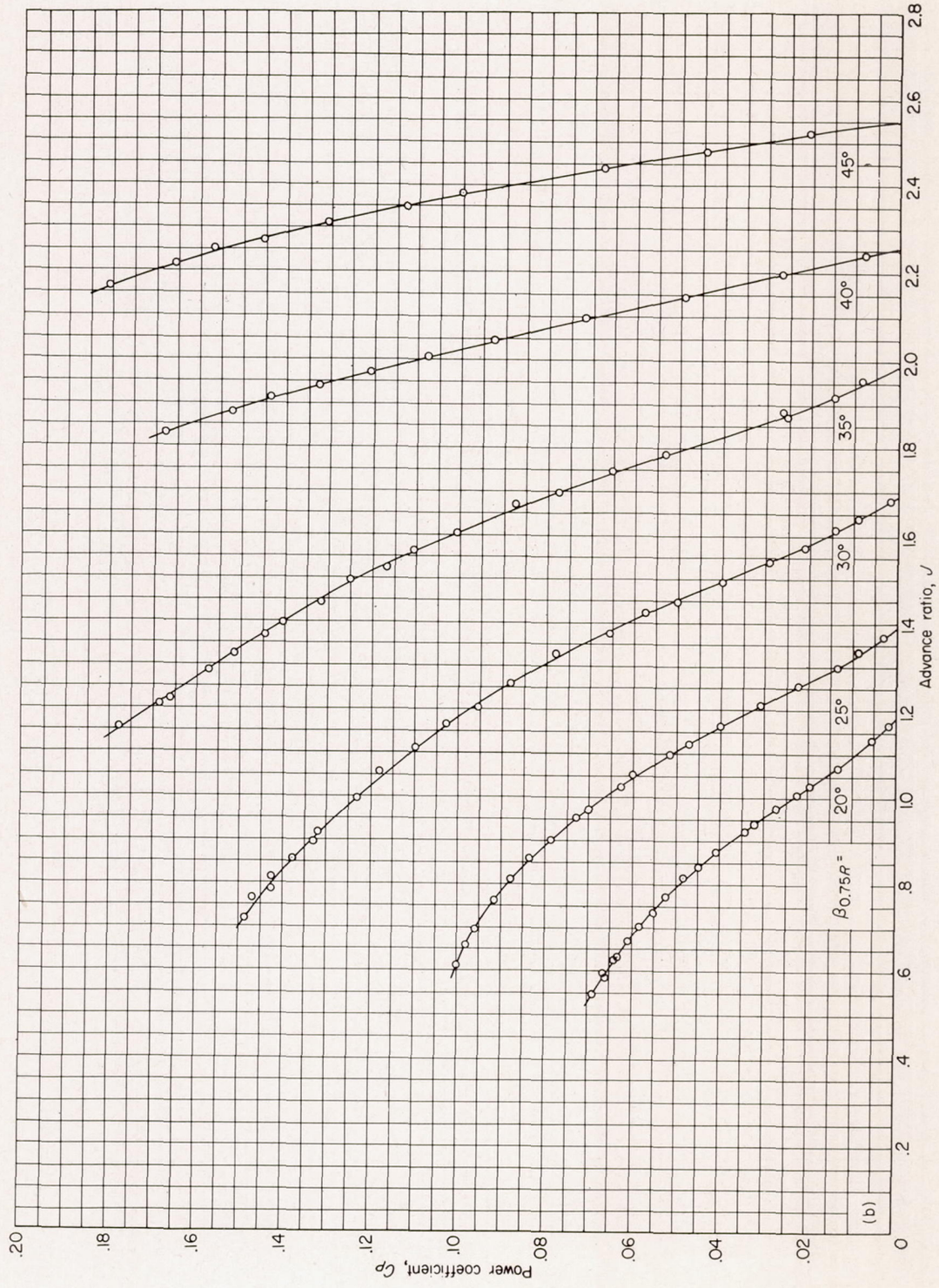

(b) Power coefficient.

FIGURE 10.—Continued.

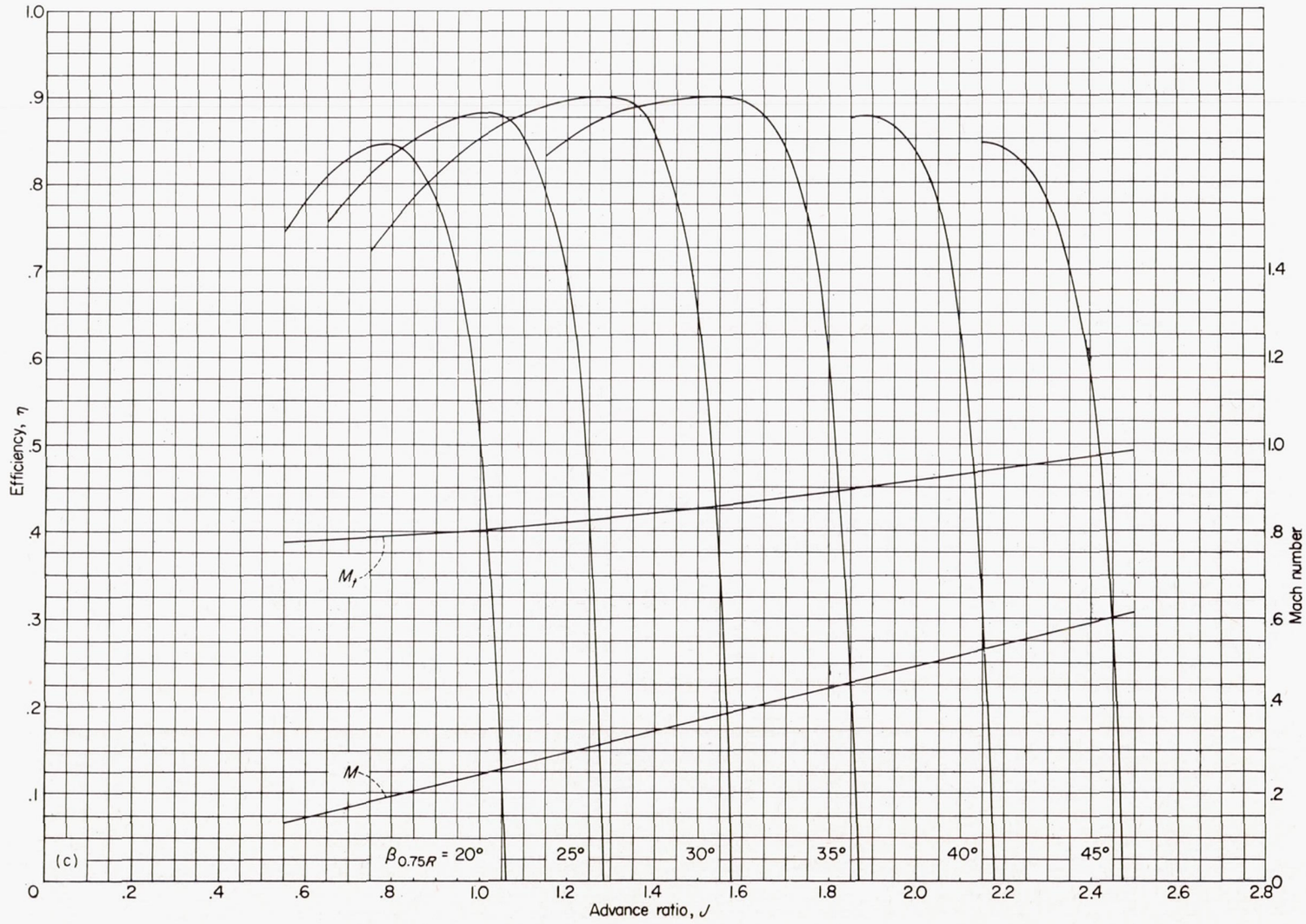

(c) Efficiency.

FIGURE 10.—Concluded.

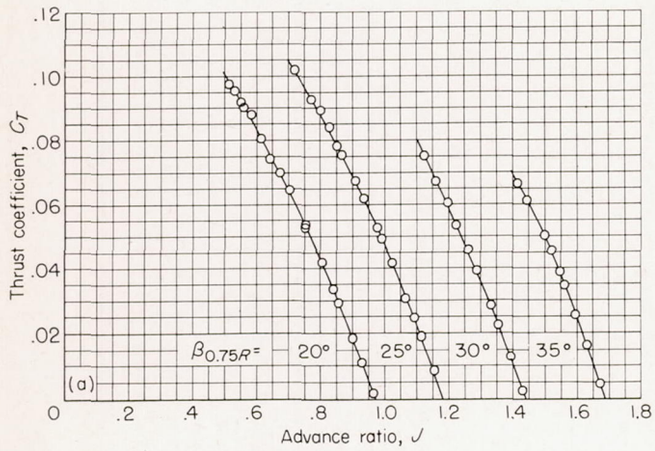

(a) Thrust coefficient.

FIGURE 11.—Characteristics of NACA 10–(10)(08)–03 propeller. Rotational speed, 2000 rpm.

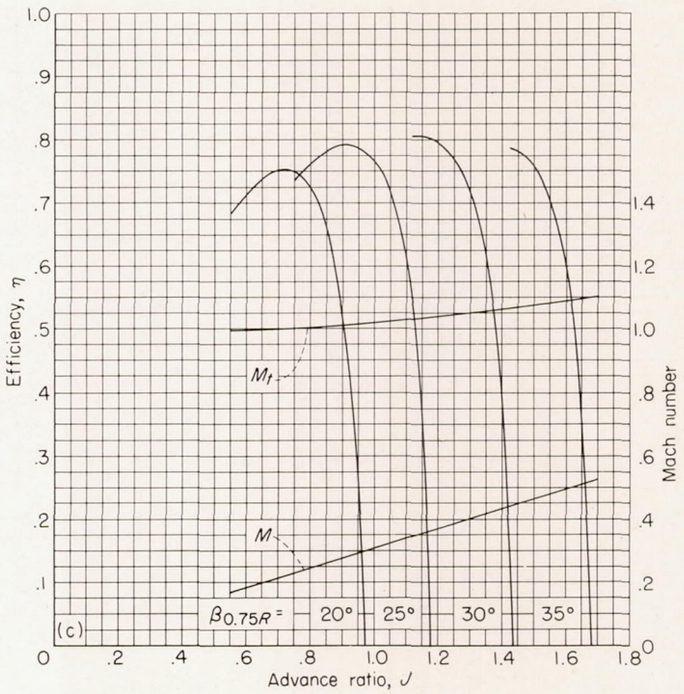

(c) Efficiency.

FIGURE 11.—Concluded.

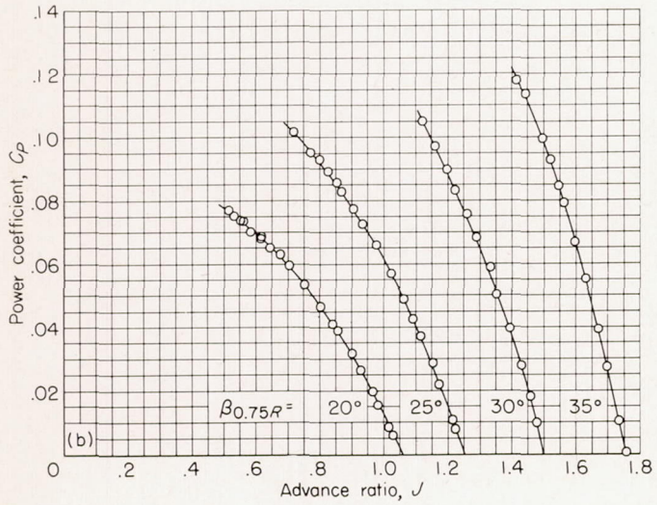

(b) Power coefficient.

FIGURE 11.—Continued.

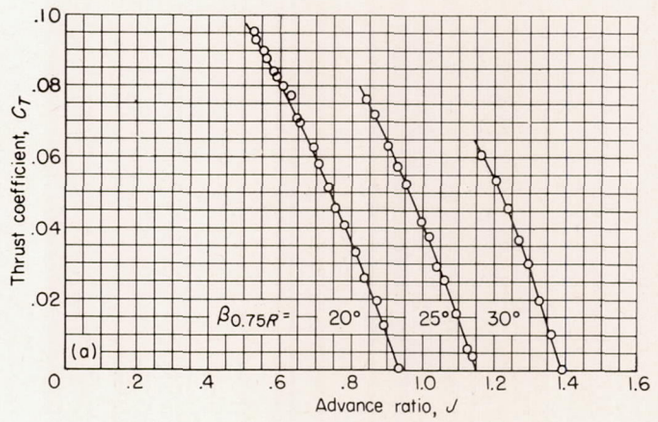

(a) Thrust coefficient.

FIGURE 12.—Characteristics of NACA 10–(10)(08)–03 propeller. Rotational speed, 2160 rpm.

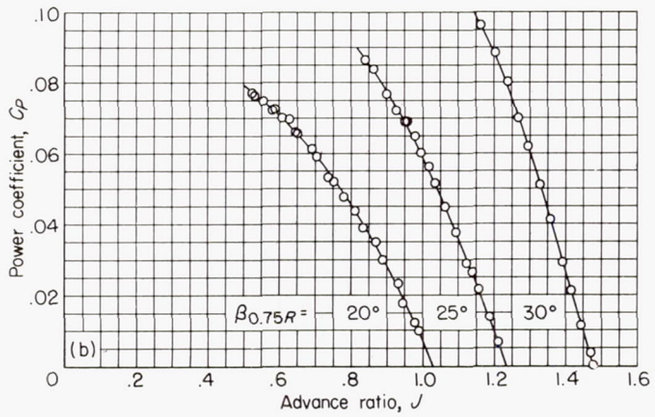

(b) Power coefficient.

FIGURE 12.—Continued.

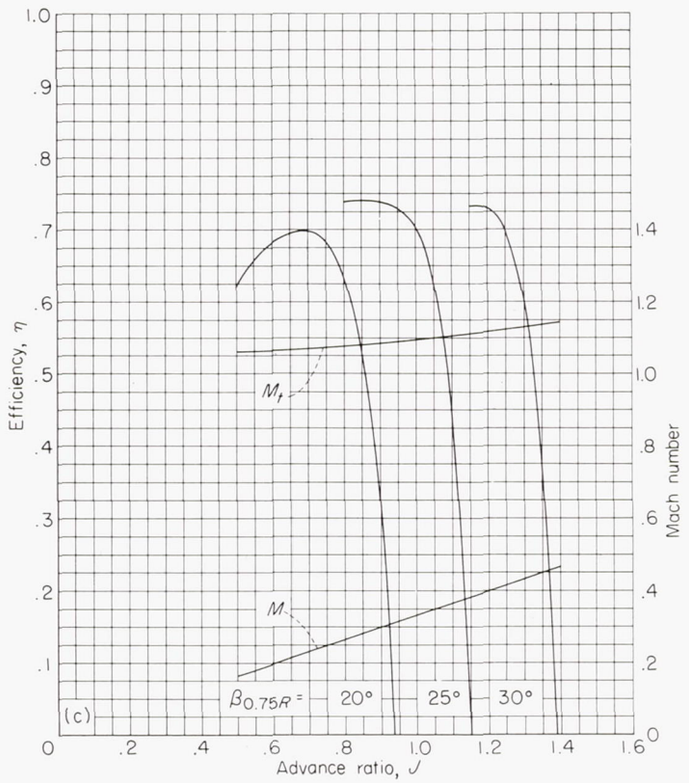

(c) Efficiency.

FIGURE 12.—Concluded.

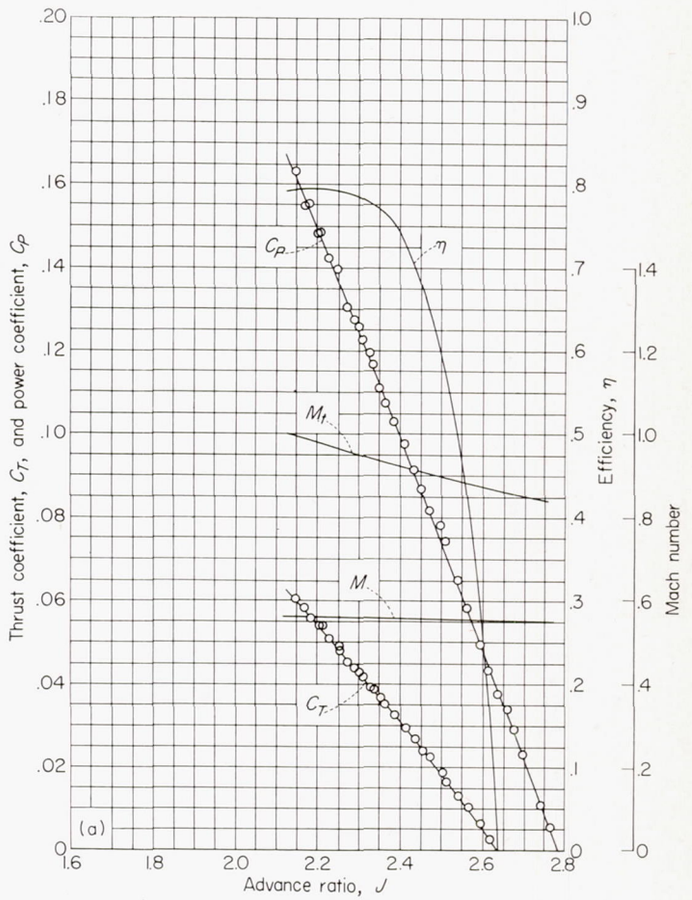

(a) Air-stream Mach number at maximum efficiency, 0.56.

FIGURE 13.—Characteristics of NACA 10–(10)(08)–03 propeller at high forward speeds. $\beta_{0.75R}=45°$.

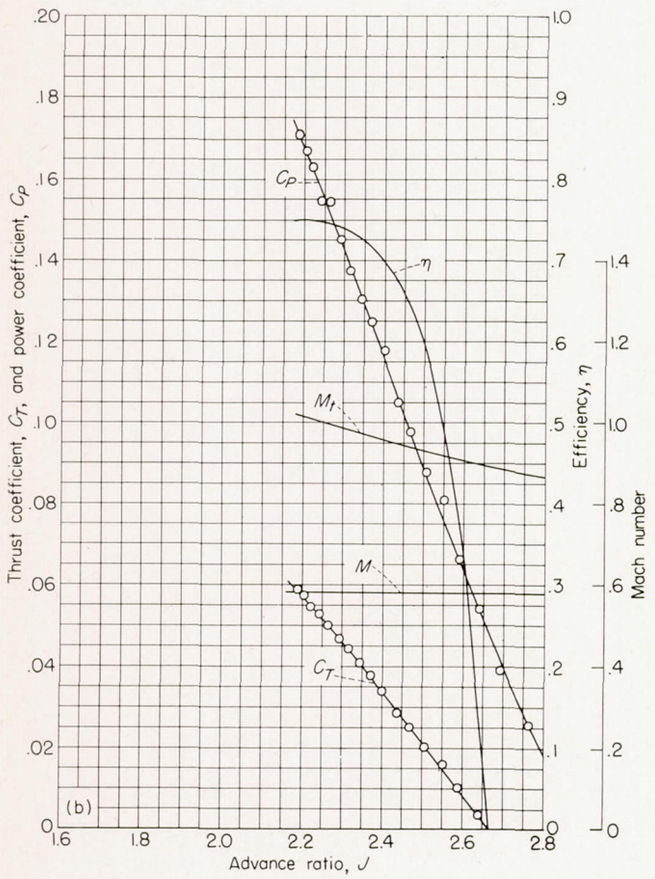

(b) Air-stream Mach number at maximum efficiency, 0.58.

FIGURE 13.—Continued.

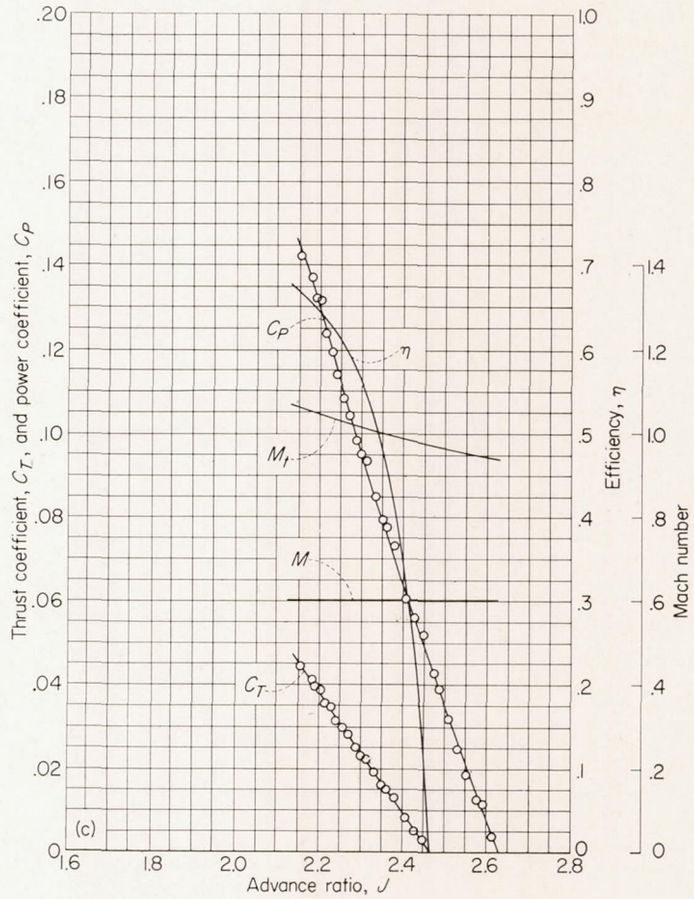

(c) Air-stream Mach number at maximum efficiency, 0.60.

FIGURE 13.—Concluded.

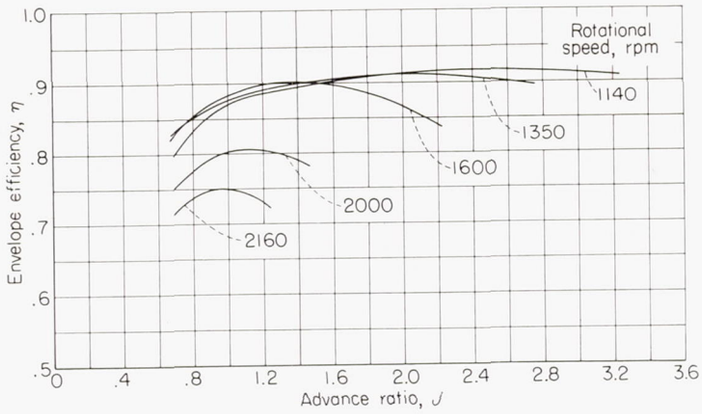

FIGURE 14.—Envelope efficiency of NACA 10–(10)(08)–03 propeller at various rotational speeds.

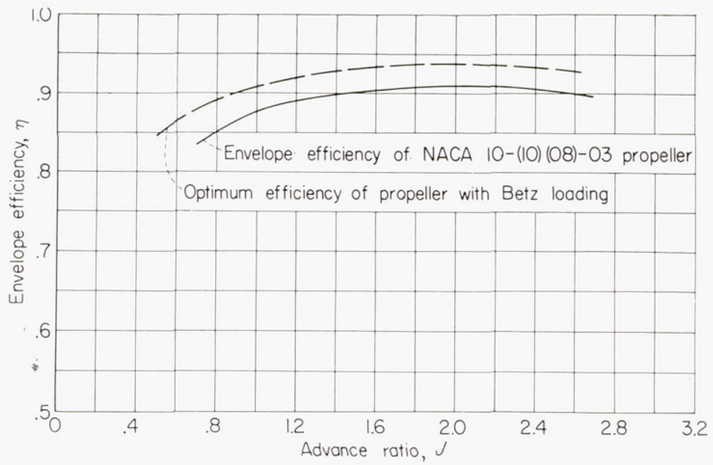

FIGURE 15.—Comparison of the envelope efficiency of NACA 10–(10)(08)–03 propeller at 1350 rpm with the optimum efficiency of a two-blade propeller with the Betz loading.

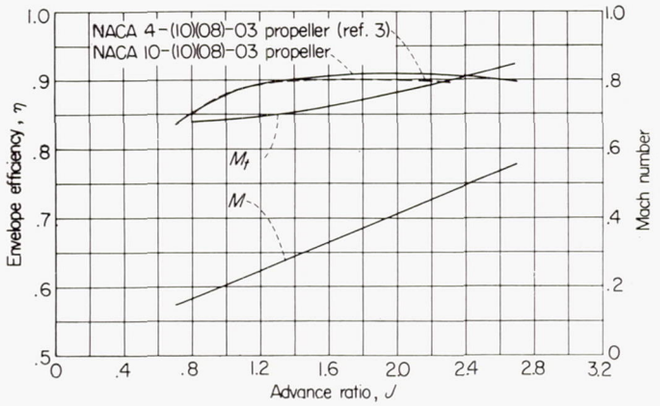

FIGURE 16.—Comparison of envelope efficiency for NACA 10–(10)(08)–03 and 4–(10)(08)–03 propellers.

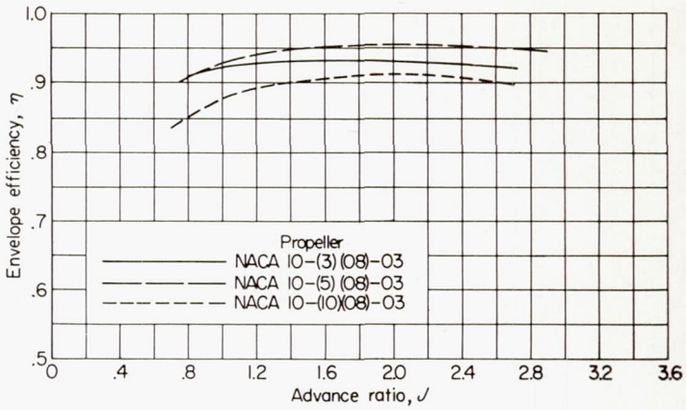

FIGURE 17.—The variation of envelope efficiency with advance ratio for propellers having different design lift coefficients. Rotational speed, 1350 rpm.

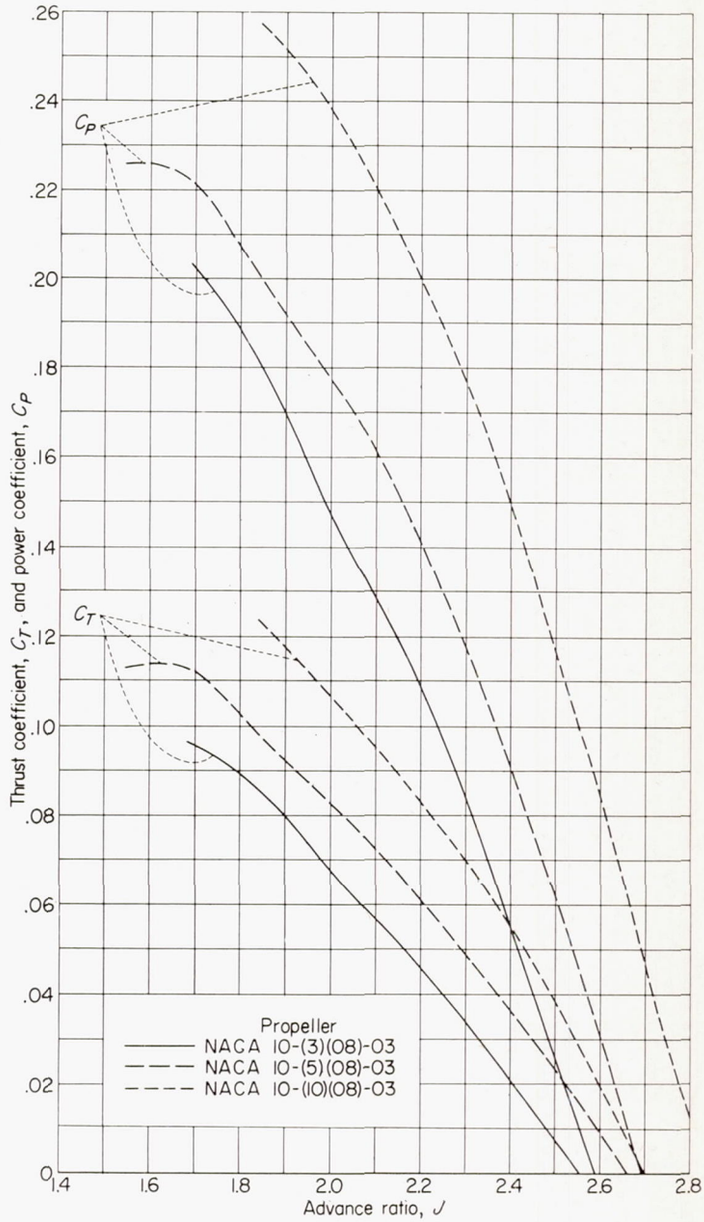

FIGURE 18.—The variation of thrust and power coefficients with advance ratio for propellers having different design lift coefficients. Rotational speed, 1350 rpm; $\beta_{0.75R}=45°$.

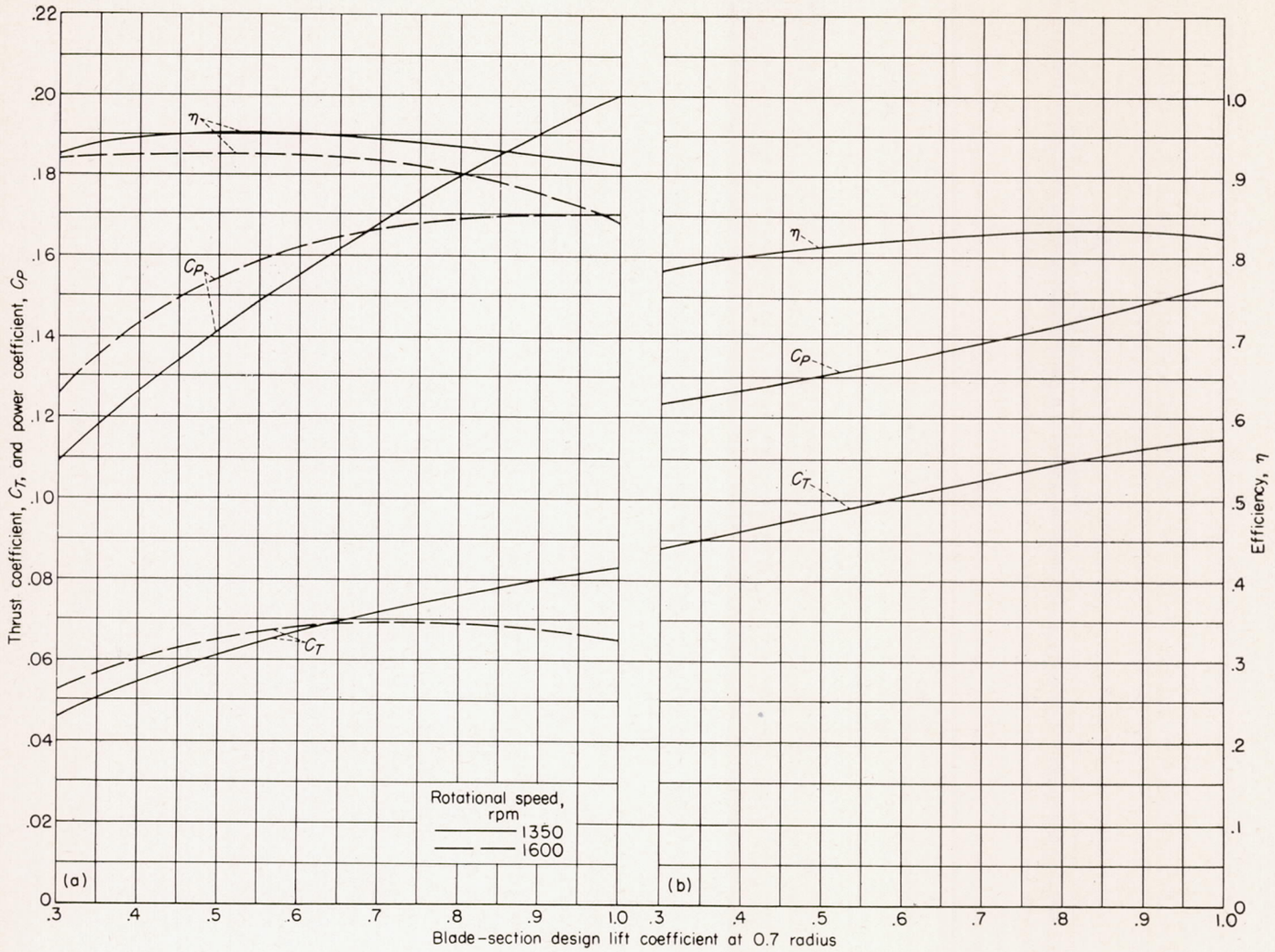

(a) $J=2.2$; $\beta_{0.75R}=45°$. (b) $J=1.1$; $\beta_{0.75R}=35°$; rotational speed, 1140 rpm.

FIGURE 19.—The effect of blade-section design lift coefficient on thrust, power, and efficiency.

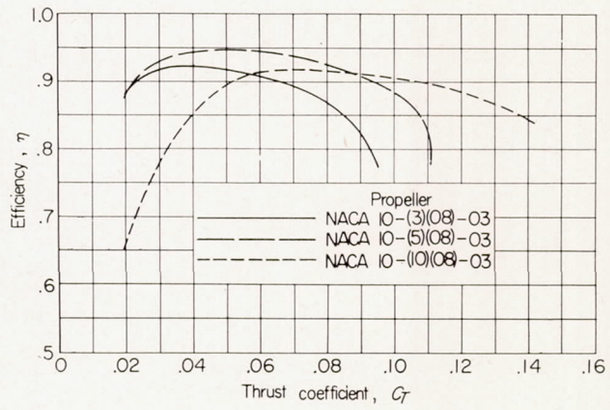

FIGURE 20.—The variation of efficiency with thrust coefficient for propellers having different design lift coefficients. Rotational speed, 1140 rpm; $\beta_{0.75R}=45°$.

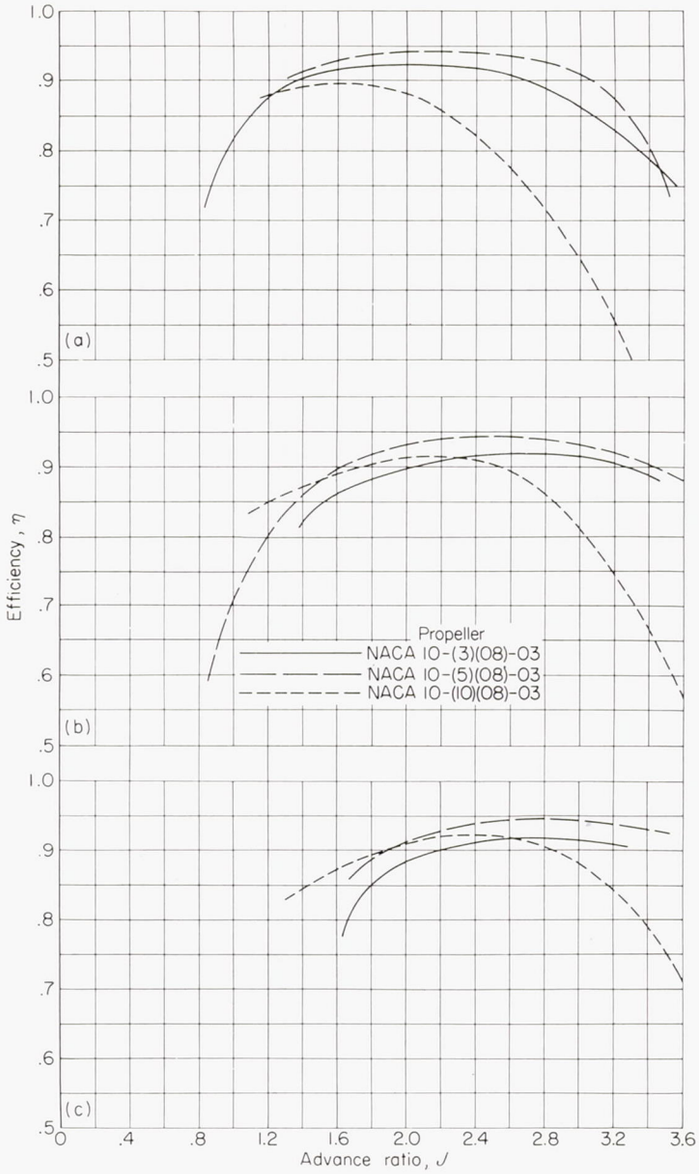

(a) $C_P = 0.10$.
(b) $C_P = 0.15$.
(c) $C_P = 0.20$.

FIGURE 21.—The efficiency of propellers having different design lift coefficients and operating at constant power coefficients and a constant rotational speed of 1140 rpm.

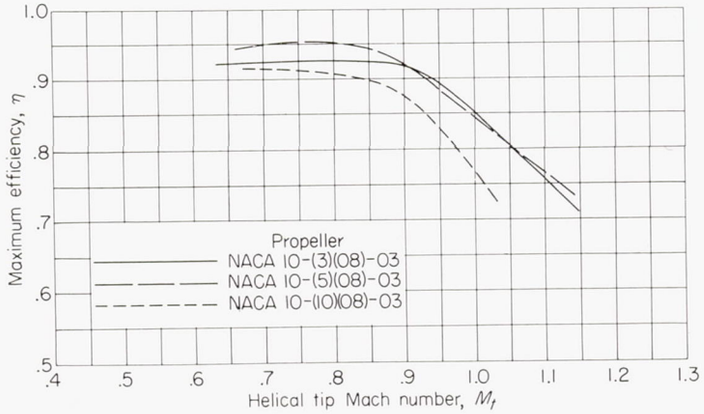

FIGURE 22.—The effect of compressibility on the maximum efficiency of propellers having different design lift coefficients. $\beta_{0.75R} = 45°$.

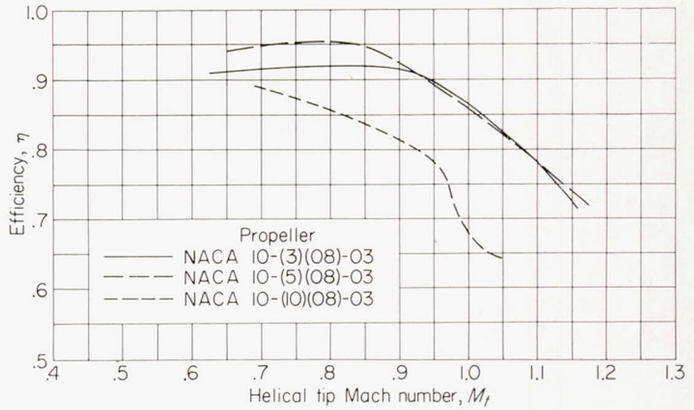

FIGURE 23.—The effect of compressibility on the efficiency of propellers having different design lift coefficients and operating at a constant power coefficient of 0.13. $\beta_{0.75R} = 45°$.

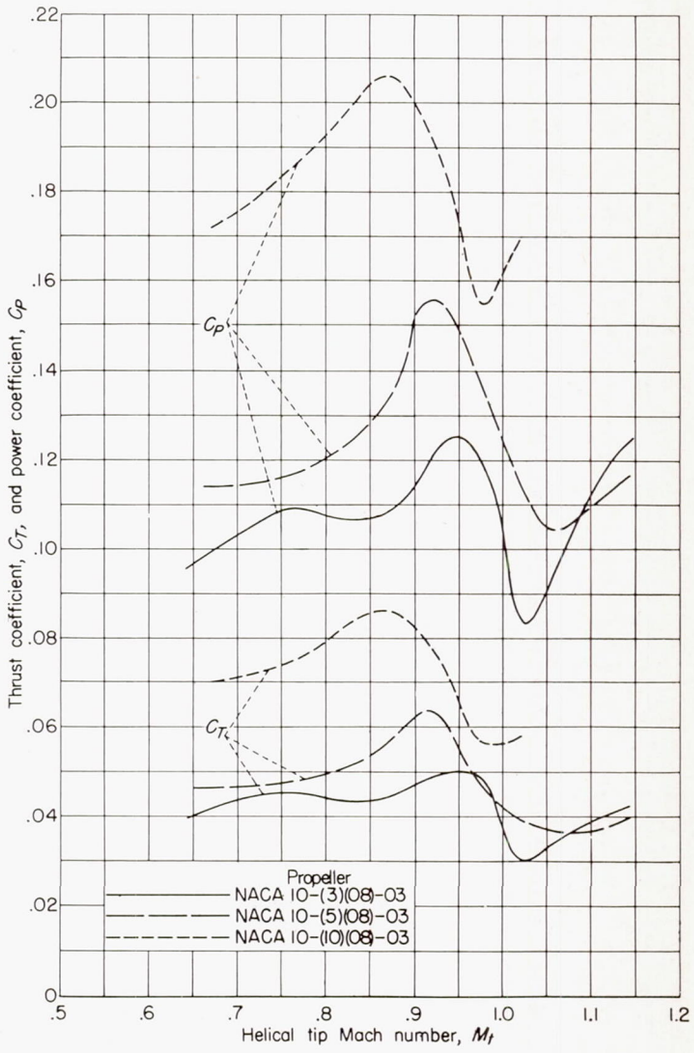

FIGURE 24.—The effect of compressibility on the thrust and power coefficients for maximum efficiency of propellers having different design lift coefficients. $\beta_{0.75R} = 45°$.

U. S. GOVERNMENT PRINTING OFFICE: 1957